DANIELLE SANTOS BRITO

FUNCTIONAL ANALYSIS OF MITOCHONDRIAL PROTEINS IN *Arabidopsis thaliana*

Thesis presented to the Universidade Federal de Viçosa as part of the requirement of the Plant Physiology Graduate Program for obtention of the degree of *Doctor Scientiae.*

VIÇOSA
MINAS GERAIS-BRAZIL
2016

Ficha catalográfica preparada pela Biblioteca Central da Universidade Federal de Viçosa - Câmpus Viçosa

T
B862f
2016

Brito, Danielle Santos, 1983-
Functional analysis of mitochondrial proteins in *Arabidopsis thaliana* / Danielle Santos Brito. – Viçosa, MG, 2016.
viii, 84f. : il. (algumas color.) ; 29 cm.

Inclui anexos.
Orientador: Adriano Nunes Nesi.
Tese (doutorado) - Universidade Federal de Viçosa.
Inclui bibliografia.

1. Proteínas. 2. *Arabidopsis thaliana. 3.* Plantas - Membrana - Transporte. 4. Mitocôndria. 5. Citologia vegetal. I. Universidade Federal de Viçosa. Departamento de Biologia Vegetal. Programa de Pós-graduação em Fisiologia Vegetal. II. Título.

CDD 22. ed. 572.6

DANIELLE SANTOS BRITO

FUNCTIONAL ANALYSIS OF MITOCHONDRIAL PROTEINS IN *Arabidopsis thaliana*

Thesis presented to the Universidade Federal de Viçosa as part of the requirement of the Plant Physiology Graduate Program for obtention of the degree of *Doctor Scientiae.*

APPROVED: 26th august of 2016

_____	_____
Carla Quinhones Godoy Soares	Fábio Murilo da Matta
_____	_____
Wagner L. Araújo	Thomas Christopher Rhys Williams

_____

Adriano Nunes Nesi
(Adviser)

ACKNOWLEDGMENTS

I would first like to thank to God, for protection and constant presence in my life.

For my lovely parents Arnaldo and Neide support, recognition and understanding of the many moments of absence.

I would to thank to my sisters by the wise counsel and sympathetic ear.

I would particularly like thank my boyfriend Roberto for supporting me and always willing to help me.

Federal University of Viçosa, in particular the Plant Biology Department, for the opportunity to develop the Plant Physiology graduation course.

Professor Adriano Nunes Nesi, who, always encouraged me to grow professionally and scientifically.

Professor Waguinho who definitely provided me with the tools that I needed to choose the right direction and successfully complete my thesis.

Professor Hans-Peter Braun for your cooperation and for all of the opportunities I was given to conduct my research.

I would like to say thank to Jennifer Senkler for supporting during my time in Germany and for your friendship.

I would like to thank my friends, especially Dalton, Franklin, Carla, Paula, David, Dôra, Izabel, Jorge Pérez, Jaciara, João Henrique for friendship, support and relaxation moments.

My sincere appreciation to all people that direct or indirectly contributed to realizing this work.

Finally, I also thank the financial support provide by Nacional Council for Scientific and Technological Development (CNPq) and Coordination for the Improvement of Higher Education Personnel (CAPES).

SUMMARY

ABSTRACT

BRITO, Danielle Santos, D.Sc., Universidade Federal de Viçosa, August, 2016. **Functional analysis of mitochondrial proteins in *Arabidopsis thaliana*.** Advisor: Adriano Nunes Nesi.

Mitochondrial carrier family (MCF) proteins catalyze the specific transport of various substrates, such as nucleotides, amino acids and cofactors. Although some of the mitochondrial transporters have been identified, many of these proteins have not yet been completely characterized. Likewise, the proteic machinery and mechanisms involved in the mitochondrial alternative respiration is still not well known. In this context, this work first presents a study of a previously identified but uncharacterized mitochondrial transporter *At*SFC1, a potential succinate/fumarate carrier. Hence, to obtain the biochemical role of *At*SFC1, we carried out substrate specificity and investigated its physiological function using 35S antisense transgenic lines in *Arabidopsis thaliana.* Briefly, the functional integration of *At*SFC1 in the cytoplasmic membrane of intact *Escherichia coli* cells reveals a high specificity for a citrate/isocitrate in a counter exchange mode. Additionally, we discussed the potential role for *At*SFC1 in the provision of intermediates of tricarboxylic acid cycle to provide carbon and energy to support growth in heterotrophic tissues. In the second part of this thesis, we investigated the function of alternative electron donors to the mitochondrial electron transport chain (mETC) during carbon deprivation as well as after the supply of amino acids. The breakdown products of branched chain amino acids can provide electrons to the mETC via the ETF/ETFQO (electron transfer flavoprotein: flavoprotein ubiquinone oxidoreductase) complex. This system is located in the mitochondria and induced at the level of transcription during stress situations. Thus, in order to obtain a comprehensive picture of how alternative respiration pathway interacts with other pathways and adjust to different cellular and metabolic requirements, we performed metabolic and physiological approaches using *Arabidopsis* cell culture ETFQO T-DNA insertion mutants. The results discussed here support that the ETF/ETFQO system is an essential pathway able to donate electrons to the ubiquinone pool. In addition,

the behavior of the respiratory complexes suggest new electrons entry points, which must be elucidated.

RESUMO

BRITO, Danielle Santos, D.Sc., Universidade Federal de Viçosa, Agosto, 2016. **Análise funcional de proteínas mitocondriais em *Arabidopsis thaliana*.** Orientador: Adriano Nunes Nesi.

A família de transportadores mitocondriais (MCF) catalisam transportes específicos de vários substratos, tais como nucleotídeos, aminoácidos e cofatores. Embora alguns dos transportadores tenham sido identificados, muitas destas proteínas ainda não foram completamente caracterizadas. Do mesmo modo, o metabolismo mitocondrial sob estresse ainda não é completamente conhecido. Neste contexto, este trabalho apresenta inicialmente um estudo de um transportador mitocondrial previamente identificado e ainda não caracterizado, designado como *At*SFC1, um potencial transportador de succinato/fumarato. Assim, para identificar a especificidade de substrato, a proteína AtSFC1 foi integrada em liposomas e ensaios bioquímicos foram realizados e para investigar a função fisiológica deste transportador, foram utilizadas plantas transgênicas de *Arabidospis thaliana* para o gene *AtSFC1,* cuja expressão foi reduzida pela técnica antisenso. Brevemente, a integração funcional do *At*SFC1 na membrana citoplasmática de células de *Escherichia coli* revelou uma especificidade para citrato/isocitrato do tipo antiporte. Além disso, discutimos o potencial papel para *At*SFC1 no fornecimento de intermediários para o ciclo ácido dos tricarboxílicos para suportar o crescimento nos tecidos heterotróficos. Na segunda parte desta tese, investigou-se a função de doadores de elétrons alternativos para a cadeia mitocondrial transportadora de elétrons (mCTE) sob deficiência de carbono, bem como após o fornecimento de aminoácidos. Os produtos de degradação de aminoácidos de cadeia ramificada podem doar elétrons para o mCTE através do complexo ETF/ETFQO (*electron transfer flavoprotein*: *flavoprotein ubiquinone oxidoreductase)*. Este sistema está localizado na mitocôndria e induzido ao nível de transcrição em situações de estresse. Assim, a fim de obter um *design* detalhado de como essa via interage com outras e como ela se ajusta a diferentes requisitos celulares e metabólicas, foram realizadas abordagens metabólicas e fisiológicas utilizando cultura de células de *Arabidopsis* mutantes com inserção de T-DNA

na região codificante do gene *ETFQO*. Os resultados são aqui discutidos, confirmam que o sistema ETF/ETFQO é uma via essencial capaz de doar elétrons para o *pool* de ubiquinona. Além disso, o comportamento dos complexos respiratórios sugere novos pontos de entrada de elétrons, os quais devem ser elucidados.

GENERAL INTRODUCTION

Mitochondrion are responsible primarily for oxidation of organic acids with oxidative phosphorylation (OXPHOS). This catabolic function is coupled with the energy production in the form of ATP (adenosine triphosphate). Mitochondrion also play roles in a wide range of processes, in which provide precursors for different and essential biosynthetic processes such as biosynthesis of amino acids, fatty acids, vitamins and cofactors (Giegé et al., 2003; Picault et al., 2004). In addition, mitochondrion are involved in photorespiration, plant cell redox and signaling, and regulatory functions such as programmed cell death (Vanlerberghe et al., 2009; Millar et al., 2011; Palmieri et al., 2011). Thus, mitochondrion need a large number of proteins to perform all these roles (Kruft et al., 2001). In this context, it has been computed that approximately 2,000-2,500 proteins are present in plant mitochondria (Millar et al., 2005). The majority of them are nuclear encoded and post-translationally transported into the organelle by complex protein import machinery (Lithgow, 2000).

Various large-scale proteomics studies consolidated a non-redundant set of 726 mitochondrial proteins in *Arabidopsis thaliana* experimentally identified (Lee et al., 2013). At present, Rao et al. (2016) collated all experimentally identified mitochondrial proteins from *Arabidopsis* added to new proteomics data presenting a list of 1005 proteins. Of the 726 identified mitochondrial proteins, approximately 22% are components of pyruvate metabolism/tricarboxylic acid (TCA) cycle and OXPHOS; and 10% are involved with transport mechanisms. Additionally, 18% of the identified proteins remain without any functional class (Lee et al., 2013). On the one hand, it is clear that the main challenge will be elucidate the set of proteins that remain without known function and its role in the plant metabolism. On the other hand, draw the mitochondrial protein composition will help us to understand better the mitochondrial metabolic processes that remain unknown.

Mitochondrial transporters abundance and function

Mitochondrial metabolism is fully integrated into cellular metabolism via a range of transporters (Linka and Weber, 2010). The outer mitochondrial membrane is permeable to several small molecules with a molecular mass of less than 4-5 kDa (Palmieri et al., 2011). On the other hand, the inner mitochondria membrane (IMM) is impermeable to most of metabolites and only small and uncharged molecules can pass through this membrane, for instance, O_2 and CO_2 (Palmieri et al., 2011).

The majority of the proteins that facilitates the transport of hydrophilic compounds across the IMM belongs to MCF (Mitochondrial Carrier Family) that are presents in different eukaryotic organisms (Picault et al., 2004). All MCF members share a tripartite structure of 100 amino acid segments each consisting of two membrane-spanning-helices separated by an extra-membrane hydrophilic loop (Picault et al., 2004; Palmieri et al., 2011). Each repeated segment contain a characteristic conserved mitochondrial energy transfer signatures (P-x-[DE]-x-[LIVAT]-[RK]-x-[LRK]-[LIVMFY]-[QGAIVM]) (PROSITE PS50920, PFAM PF00153 and IPR00193). However, it is important to note that not all carriers belonging to the MCF family are targeted to the mitochondria after translation of RNA into protein in the cytosol (Palmieri et al., 2009; Palmieri and Pierri, 2010). Recent molecular and biochemical studies revealed that MCFs proteins are also localized in plant plastids (Bouvier et al., 2006; Kirchberger et al., 2008; Palmieri et al., 2009), peroxisomes (Palmieri et al., 2001; Linka et al., 2008) and the endoplasmic reticulum of *Arabidopsis thaliana* (Leroch et al., 2008).

Depending on the type of substrates they transport, MCF members can be divided into four major classes or groups. The first subfamily comprises nucleotide and nucleotide derivate transporters; the second mediates the passage of di and tricarboxylates or keto acids. Amino acid carriers and carnitine/acylcarnitine carriers are associate to a third functional group and the fourth subdivision represents the transporters with other substrates like H^+ passage or phosphate (Palmieri et al., 2011). It is important to highlight that some substrates, and even certain defining substrates, are transported by

more than one subfamily. Moreover, some subfamilies may transport additional, yet untested substrates (Marobbio et al., 2008).

Identification of the substrate specificity of new MCFs is a laborious work. The best strategy is heterologous gene expression in *Escherichia coli* and reconstitution of purified recombinant carriers into liposomes (Fiermonte et al., 1993). The most of the MCFs has been cloned and investigated at the molecular and biochemical level (Picault et al., 2002; Leroch et al., 2005; Bouvier et al., 2006; Palmieri et al., 2008a; 2008b) using these methods. The MCF members can be also identified by proteomics studies, however their substrate specificity can not be identified by these strategies. The method *complexome profiling* combines classical blue-native electrophoresis (BNE) with modern proteomic methods of quantitative mass spectrometry and hierarchical clustering to identify known and unknown macromolecular protein complexes (Millar and Heazlewood, 2003; Millar et al., 2005; Taylor et al., 2011). Recently, by this method, was found the carrier *At*SFC1 (At5g01340), of unknown function (Braun et al, data not published). This carrier is a homologous of succinate/fumarate carrier (ACR1) from *Saccharomyces cerevisiae.* Studies of functional complementation performed in yeast mutants deficient in the expression of *ACR1* gene, suggest that *At*SFC1 also act as cytosol succinate carrier into the mitochondrial matrix in exchange of fumarate, which is transported to the cytosol (Catoni et al., 2003). Additionally, they also demonstrate a greater expression of the *At*SFC1 in roots and closed flowers, and in less extent, in open flowers, sink and source leaves and stems. The gene expression studies suggest a substantially constitutive expression of *At*SFC1 in various tissues and at different stages of development.

Although, it has been hypothesize the probably involvement of the *At*SFC1 in plant metabolism, until now, a single work was carried out aiming to understand the physiological contribution of this transporter in plants. Notwithstanding, this characterization performed in *A. thaliana* only allowed the identification of tissues and plant organs where this protein is expressed (Catoni et al., 2003). In this context, it is important elucidate the physiological role of this protein, once that seems to be involved in crucial events of the plant life cycle.

Alternative respiratory pathway

The classical respiratory process in plants involves a combination of different metabolic pathways that includes glycolysis, tricarboxilic acids (TCA) cycle and oxidative phosphorylation (Millar et al., 2011). These processes are very important in a variety of physiological functions as ATP generation, provide of carbon skeletons for biosynthetic processes, photorespiration and others (van Dongen et al., 2011). In addition, the respiration is mostly dependent of carbohydrate oxidation. However, in situations where carbohydrates level is decreased, alternative substrates such proteins, lipids and chlorophylls can be used for maintenance of ATP production (Ishizaki et al., 2005; 2006; Araújo et al., 2010). Among these alternative substrates, it has been demonstrated that amino acids can act as electron donor to support respiration (Ishizaki et al., 2005; 2006; Araújo et al., 2010). The use of amino acids associated with energy production occurs through a distinct route that differs from the classical pathway of respiration. This alternative pathway of respiration is performed by the Electron transfer flavoprotein: flavoprotein ubiquinone oxidoreductase (ETF/ETFQO) system (Watmough and Frerman, 2010).

In *Arabidopsis thaliana*, the ETF/ETFQO system was identified in mitochondria by the use of gel-based or liquid chromatography tandem mass spectrometry mitochondrial proteomic analysis (Heazlewood et al., 2004) and demonstrated to be induced at the level of transcription during dark-induced senescence (Buchanan-Wollaston et al., 2005). The ETFQO is associated with the IMM and ETF is located in the mitochondrial matrix. The ETFQO accepts electrons from ETF, which serves as an obligatory electron acceptor for mitochondrial matrix flavoprotein dehydrogenases. Subsequently, reduced ETF is then re-oxidized by the ETFQO, which delivers electrons to the main respiratory chain via ubiquinone reduction (Frerman, 1987).

In mammals, eleven dehydrogenases able to donate electrons to ETF/ETFQO system were identified. By contrast, in plants, to date, only two enzymes were identified, 2-hydroxyglutarate dehydrogenase (D-2HGDH) and isovaleryl-CoA dehydrogenase (IVDH) associated with the ETF/ETFQO system (Engqvist et al., 2009; Araújo et al., 2010). D-2HGDH located in the

mitochondrial matrix, catalyze the oxidation of 2-hydroxyglutarate into 2-oxoglutarate (Engqvist et al., 2009). In addition, IVDH, another mitochondrial matrix enzyme, are linked to the degradation of the branched chain amino acids (BCAA) (Ding et al., 2012).

The role of this pathway in plant had been characterized by use of loss-function *Arabidopsis* mutants (Ishizaki et al., 2005; 2006; Araújo et al., 2010; Peng et al., 2015). Mutant plants in this alternative pathway showed accelerated senescence as compared to wild type (Ishizaki et al., 2005; 2006; Araújo et al., 2010; Pires et al., 2016). In addition, metabolic profiling revealed that all mutants accumulated several amino acids as well as phytanoyl-CoA, a chlorophyll degradation product (Araújo et al., 2010).

Despite all the studies performed so far (Palmieri et al., 1997; Catoni et al., 2003; Ishizaki et al., 2005; 2006; Araújo et al., 2010) our knowledge about the physiological role of the mitochondrial carries is still scarce as well as the proteic machinery and mechanisms involved in the alternative respiration. Thereby, this work focused on the function of mitochondrial transporters and the role of alternative electron donors to the mETC. Thus, this study is divided in two chapters. In the first chapter, the main goal was to characterize the physiological role of the *At*SFC1, a potential succinate/fumarate carrier member of the MC family. For this, we investigated the biochemical properties and substrate specificity. In addition, by qRT-PCR analysis we performed tissue-specific expression. Finally, we used 35S *At*SFC1 antisense transgenic plants of *A. thaliana* carried out a series of experiments to characterize the physiological role of this carrier in the plant metabolism. In the second chapter, the main goal was investigate how exactly the OXPHOS system can affect the respiratory complexes following carbohydrate starvation on as well as when supplemented with BCAA. For this, metabolic and physiological approaches were carried out using *Arabidopsis* cell culture ETFQO T-DNA insertion mutants. The results discussed here support that the ETF/ETFQO system is an essential pathway able to donate electrons to the mETC and that amino acids are alternative substrates maintaining respiration under carbon starvation.

REFERENCES

Araújo WL, Ishizaki K, Nunes-Nesi A, Larson TR, Tohge T, Krahnert I, Witt S, Obata T, Schauer N, Graham I a, et al (2010) Identification of the 2-hydroxyglutarate and isovaleryl-CoA dehydrogenases as alternative electron donors linking lysine catabolism to the electron transport chain of Arabidopsis mitochondria. Plant Cell **22**: 1549–63

Bouvier F, Linka N, Isner J-C, Mutterer J, Weber APM, Camara B (2006) Arabidopsis SAMT1 defines a plastid transporter regulating plastid biogenesis and plant development. Plant Cell **18**: 3088–105

Buchanan-Wollaston V, Page T, Harrison E, Breeze E, Lim PO, Nam HG, Lin JF, Wu SH, Swidzinski J, Ishizaki K, et al (2005) Comparative transcriptome analysis reveals significant differences in gene expression and signalling pathways between developmental and dark/starvation-induced senescence in Arabidopsis. Plant J **42**: 567–585

Catoni E, Schwab R, Hilpert M, Desimone M, Schwacke R, Flügge UI, Schumacher K, Frommer WB (2003) Identification of an Arabidopsis mitochondrial succinate-fumarate translocator. FEBS Lett **534**: 87–92

Ding G, Che P, Ilarslan H, Wurtele ES, Nikolau BJ (2012) Genetic dissection of methylcrotonyl CoA carboxylase indicates a complex role for mitochondrial leucine catabolism during seed development and germination. Plant J **70**: 562–577

van Dongen JT, Gupta KJ, Ramírez-Aguilar SJ, Araújo WL, Nunes-Nesi A, Fernie AR (2011) Regulation of respiration in plants: A role for alternative metabolic pathways. J Plant Physiol **168**: 1434–1443

Engqvist M, Drincovich MF, Flügge UI, Maurino VG (2009) Two D-2-hydroxy-acid dehydrogenases in arabidopsis thaliana with catalytic capacities to participate in the last reactions of the methylglyoxal and β-oxidation pathways. J Biol Chem **284**: 25026–25037

Fiermonte G, Walker JE, Palmieri F (1993) Abundant bacterial expression and reconstitution of an intrinsic membrane-transport protein from bovine mitochondria. Biochem J **294**: 293–299

Frerman FE (1987) Reaction of electron-transfer flavoprotein ubiquinone oxidoreductase with the mitochondrial respiratory chain. Biochim Biophys Acta - Bioenerg **893**: 161–169

Giegé P, Heazlewood JL, Roessner-Tunali U, Millar AH, Fernie AR, Leaver CJ, Sweetlove LJ (2003) Enzymes of glycolysis are functionally associated with the mitochondrion in Arabidopsis cells. Plant Cell **15**: 2140–51

Heazlewood JL, Tonti-Filippini JS, Gout AM, Day DA, Whelan J, Harvey Millar A (2004) Experimental Analysis of the Arabidopsis Mitochondrial Proteome Highlights Signaling and Regulatory Components, Provides Assessment of Targeting Prediction Programs, and Indicates Plant-

Specific Mitochondrial Proteins. Plant Cell **16**: 241–256

Ishizaki K, Larson TR, Schauer N, Fernie AR, Graham IA, Leaver CJ (2005) The critical role of Arabidopsis electron-transfer flavoprotein:ubiquinone oxidoreductase during dark-induced starvation. Plant Cell **17**: 2587–2600

Ishizaki K, Schauer N, Larson TR, Graham IA, Fernie AR, Leaver CJ (2006) The mitochondrial electron transfer flavoprotein complex is essential for survival of Arabidopsis in extended darkness. Plant J **47**: 751–760

Kirchberger S, Tjaden J, Ekkehard Neuhaus H (2008) Characterization of the Arabidopsis Brittle1 transport protein and impact of reduced activity on plant metabolism. Plant J **56**: 51–63

Kruft V, Eubel H, Jänsch L, Werhahn W, Braun HP (2001) Proteomic approach to identify novel mitochondrial proteins in Arabidopsis. Plant Physiol **127**: 1694–710

Lee CP, Taylor NL, Millar AH (2013) Recent Advances in the Composition and Heterogeneity of the Arabidopsis Mitochondrial Proteome. Front Plant Sci **4**: 4

Leroch M, Kirchberger S, Haferkamp I, Wahl M, Neuhaus HE, Tjaden J (2005) Identification and characterization of a novel plastidic adenine nucleotide uniporter from Solanum tuberosum. J Biol Chem **280**: 17992–18000

Leroch M, Neuhaus HE, Kirchberger S, Zimmermann S, Melzer M, Gerhold J, Tjaden J (2008) Identification of a novel adenine nucleotide transporter in the endoplasmic reticulum of Arabidopsis. Plant Cell **20**: 438–451

Linka N, Theodoulou FL, Haslam RP, Linka M, Napier JA, Neuhaus HE, Weber APM (2008) Peroxisomal ATP import is essential for seedling development in Arabidopsis thaliana. Plant Cell **20**: 3241–3257

Linka N, Weber APM (2010) Intracellular metabolite transporters in plants. Mol Plant **3**: 21–53

Lithgow T (2000) Targeting of proteins to mitochondria. FEBS Lett **476**: 22–26

Marobbio CMT, Giannuzzi G, Paradies E, Pierri CL, Palmieri F (2008) alpha-Isopropylmalate, a leucine biosynthesis intermediate in yeast, is transported by the mitochondrial oxalacetate carrier. J Biol Chem **283**: 28445–53

Millar AH, Heazlewood JL (2003) Genomic and proteomic analysis of mitochondrial carrier proteins in Arabidopsis. Plant Physiol **131**: 443–53

Millar AH, Heazlewood JL, Kristensen BK, Braun H-P, Møller IM (2005) The plant mitochondrial proteome. Trends Plant Sci **10**: 36–43

Millar AH, Whelan J, Soole KL, Day DA (2011) Organization and regulation of mitochondrial respiration in plants. Annu Rev Plant Biol **62**: 79–104

Palmieri F, Pierri CL (2010) Structure and function of mitochondrial carriers -

Role of the transmembrane helix P and G residues in the gating and transport mechanism. FEBS Lett **584**: 1931–1939

Palmieri F, Pierri CL, De Grassi A, Nunes-Nesi A, Fernie AR (2011) Evolution, structure and function of mitochondrial carriers: A review with new insights. Plant J **66**: 161–181

Palmieri F, Rieder B, Ventrella A, Blanco E, Do PT, Nunes-Nesi A, Trauth a U, Fiermonte G, Tjaden J, Agrimi G, et al (2009) Molecular identification and functional characterization of Arabidopsis thaliana mitochondrial and chloroplastic NAD+ carrier proteins. J Biol Chem **284**: 31249–31259

Palmieri L, Lasorsa FM, De Palma A, Palmieri F, Runswick MJ, Walker JE (1997) Identification of the yeast ACR1 gene product as a succinate-fumarate transporter essential for growth on ethanol or acetate. FEBS Lett **417**: 114–118

Palmieri L, Picault N, Arrigoni R, Besin E, Palmieri F, Hodges M (2008a) Molecular identification of three Arabidopsis thaliana mitochondrial dicarboxylate carrier isoforms: organ distribution, bacterial expression, reconstitution into liposomes and functional characterization. Biochem J **410**: 621–629

Palmieri L, Rottensteiner H, Girzalsky W, Scarcia P, Palmieri F, Erdmann R (2001) Identification and functional reconstitution of the yeast peroxisomal adenine nucleotide transporter. EMBO J **20**: 5049–5059

Palmieri L, Santoro A, Carrari F, Blanco E, Nunes-Nesi A, Arrigoni R, Genchi F, Fernie AR, Palmieri F (2008b) Identification and Characterization of ADNT1, a Novel Mitochondrial Adenine Nucleotide Transporter from Arabidopsis,. Plant Physiol **148**: 1797–1808

Peng C, Uygun S, Shiu S-H, Last RL (2015) The Impact of the Branched-Chain Ketoacid Dehydrogenase Complex on Amino Acid Homeostasis in Arabidopsis. Plant Physiol **169**: 1807–1820

Picault N, Hodges M, Palmieri L, Palmieri F (2004) The growing family of mitochondrial carriers in Arabidopsis. Trends Plant Sci **9**: 138–146

Picault N, Palmieri L, Pisano I, Hodges M, Palmieri F (2002) Identification of a novel transporter for dicarboxylates and tricarboxylates in plant mitochondria: Bacterial expression, reconstitution, functional characterization, and tissue distribution. J Biol Chem **277**: 24204–24211

Pires M V., Pereira Júnior AA, Medeiros DB, Daloso DM, Pham PA, Barros KA, Engqvist MKM, Florian A, Krahnert I, Maurino VG, et al (2016) The influence of alternative pathways of respiration that utilize branched-chain amino acids following water shortage in Arabidopsis. Plant, Cell Environ **39**: 1304–1319

Rao RSP, Salvato F, Thal B, Eubel H, Thelen JJ, Møller IM (2016) The proteome of higher plant mitochondria. Mitochondrion. doi: 10.1016/j.mito.2016.07.002

Taylor NL, Heazlewood JL, Millar AH (2011) The Arabidopsis thaliana 2-D gel mitochondrial proteome: Refining the value of reference maps for assessing protein abundance, contaminants and post-translational modifications. Proteomics **11**: 1720–1733

Vanlerberghe GC, Cvetkovska M, Wang J (2009) Is the maintenance of homeostatic mitochondrial signaling during stress a physiological role for alternative oxidase? Physiol Plant **137**: 392–406

Watmough NJ, Frerman FE (2010) The electron transfer flavoprotein: Ubiquinone oxidoreductases. Biochim Biophys Acta - Bioenerg **1797**: 1910–1916

CHAPTER 1

Functional characterization of the *At*SFC1 mitochondrial carrier in *Arabidopsis thaliana*

ABSTRACT

BRITO, Danielle Santos, D.Sc., Universidade Federal de Viçosa, August, 2016. **Functional characterization of the *At*SFC1 mitochondrial carrier in *Arabidopsis thaliana*.** Advisor: Adriano Nunes Nesi.

In *Arabidopsis thaliana* genome one homologue of the yeast mitochondrial ACR1 carrier, assumed as a potential succinate/fumarate carrier has been found. This transporter has been designated as *At*SFC1 (**S**uccinate/**F**umarate **C**arrier) and belongs to the mitochondrial carrier protein (MCF) family. Previous functional complementation analysis of yeast deficient SFC1 mutants, ACR1 mutant, indicated that *At*SFC1 can transport succinate from the cytosol to the mitochondrial matrix through the mitochondrial inner membrane in exchange of fumarate. However, the biochemical and physiological role of this transporter in plants were not performed in details. To further investigate the role of SFC1 in plants, we produced heterologous expression in *Escherichia coli* followed by purification, reconstitution in proteoliposomes, and uptake experiments. Surprisingly, this analysis revealed that *At*SFC1 exhibit higher affinity for citrate and isocitrate instead of succinate and transport this compound in a counter exchange mode. qRT-PCR and *in silico* expression analysis indicated that *At*SFC1 gene is expressed mainly in heterotrophic tissues. To further investigate the SFC1 role in plants we generated 35S- SFC1 antisense transgenic lines. The reduced expression of SFC1 carrier in transgenic lines reduced germination independent of the addition of sucrose as a carbon source. Furthermore, in leaves, the lines displayed altered CO_2 assimilation rate and carbon metabolism. In addition, lower expression of SFC1 impact root growth. Taken together these findings are discussed in the context of a potential role for *At*SFC1 in the provision of intermediates of TCA cycle to provide carbon and energy to support growth in heterotrophic tissues.

Key words: Carrier, citrate, fumarate, metabolism, mitochondria, succinate.

INTRODUCTION

The cellular compartmentalization is a distinctive feature of eukaryotic cell metabolism (Farre et al., 2001; Lunn, 2007). Despite of physically and biochemically distinct, these compartments and their metabolic contents are connected by the transport of metabolites (Krueger et al., 2011). Thus, the proper functioning of the cellular metabolism, metabolic processes require rapid exchange of molecules between different cellular compartments that depend on the supply and demand of metabolic precursors (Linka and Weber, 2010). However, some cells membranes such as inner mitochondria membrane is impermeable of the most of metabolites and only small molecules can pass through this membrane, for instance O_2 and CO_2. Therefore, it is necessary the existence of specific proteins that carry out the import and export of metabolites through these membranes (Lunn, 2007; Sze et al., 2014).

The majority of the proteins that facilitates the transport of hydrophilic compounds across the IMM belongs to MCF (Mitochondrial Carrier Family). All members of this family have a common structural feature, which is composed of a primary structure of three tandemly repeated homologous domains with about 100 amino acids in length (Palmieri, 1994). Each domain contains two transmembrane proteins α-helix separated by an extramembrane with one hydrophilic loop (Picault et al., 2004; Palmieri et al., 2011). These proteins have a molecular mass between 30-34 kDa and can catalyze the transport of a wide range of molecules in size and structure, such as nucleotides, amino acids, dicarboxylates, cofactors, phosphate or H^+ (Millar and Heazlewood, 2003; Picault et al., 2004; Palmieri and Pierri, 2010; Palmieri et al., 2011).

The use of direct and reverse genetics in *Arabidopsis thaliana* has provided greater understanding of the physiological role of some MCF transporters in plants (Palmieri, 2004; Palmieri et al., 2008b; Palmieri et al., 2009). However, the physiological role of the majority of them remains unknown (Palmieri et al., 2011). Among the hitherto characterized carriers can be highlighted those involved with the respiratory chain complexes and the proton motive force. ADP/ATP carrier (AAC), which catalyzes the efflux of ATP

to the cytosol in a co-system-transport with ADP (Klingenberg, 2008); adenine nucleotide transporter (ADNT1), a protein that drive the ATP transport from the mitochondrial matrix to the intermembrane space in exchange for cytosolic AMP (Palmieri et al., 2008b). Furthermore, there are the dicarboxylic acids carriers (DIC), that in plants could play an important role in several metabolic processes including primary amino acid synthesis (ammonium assimilation), fatty acid metabolism (mobilization during seed germination), gluconeogenesis and isoprenoid biosynthesis. They transport a wide range of dicarboxylic acids including malate, oxaloacetate and succinate as well as phosphate, sulfate and thiosulfate at high rates, whereas 2-oxoglutarate was revealed to be a very poor substrate (Palmieri et al., 2008a). A similar carrier to the DIC is the dicarboxylate/tricarboxylate carrier (DTC), was shown to mediate an electroneutral transport of different single protonated tricarboxylates (citrate, isocitrate, and aconitate) in exchange with a broad variety of unprotonated dicarboxylates (2-oxoglutarate, oxaloacetate, malate, maleate, succinate, and malonate (Picault et al., 2002).

In *Arabidopsis thaliana* a homologous of ACR1 from *Saccharomyces cerevisiae*, has been identified, cloned and named *At*SFC1 (Catoni et al., 2003). However, its functional role in plants remains unknown. In functional complementation studies performed in yeast mutants deficient in the expression of *ACR1* gene, suggest that *At*SFC1 act as cytosol succinate carrier into the mitochondrial matrix in exchange of fumarate, which is transported to the cytosol (Catoni et al., 2003). The expression *At*SFC1 gene in *A. thaliana* occurs in many organs, such as source and sink leaves, roots, stems, as well as open and closed flowers (Catoni et al., 2003) as well as in two day-old dark grown seedlings, which declined in cotyledons during further development (Catoni et al., 2003).

The *At*SFC1 expression pattern in early germination of Arabidopsis seeds suggests its relation in export of fumarate for gluconeogenesis during lipid mobilization (Eastmond and Graham, 2001; Kunze et al., 2006; Graham, 2008). Interestingly, the expression of *At*SFC1 in mature leaves cannot be explained solely by the increase in the activity of the glyoxylate cycle, as observed in seeds. Although had been detected ICL activity in mature leaves of several species including wheat, maize (Godavari et al., 1973), pea (Hunt

and Fletcher, 1977) and tobacco (Zelitch, 1988) the function of the glyoxylate cycle in these tissues is still unknown.

Despite the functional complementation of yeast ACR1 mutant suggest that *At*SFC1 is probably a succinate/fumarate transporter (Catoni et al., 2003), a biochemical evidence for that remains to be found. Moreover, it had been demonstrate that the ACR1 also recognizes oxoglutarate, oxalacetate, malate, phosphoenolpyruvate, citrate or isocitrate (Palmieri et al., 1997). Therefore, it is likely that *At*SFC1 transports other substrates besides succinate and fumarate. Thus, it is necessary to verify the biochemical and physiological role of this protein in plants. Thereby, biochemical and physiological studies are essential to a greater understanding of how and to what extend the *At*SFC1 carrier has a role in cell metabolism. For this reason, in this study we investigated the biochemical properties of *At*SFC1 protein after proteoliposome reconstitution as well as tissue-specific expression in *Arabidopsis* plants. Our results of functional integration of *At*SFC1 protein in the cytoplasmic membrane of intact *Escherichia coli* revealed a high specificity for a citrate/isocitrate antiport. Reconstituted *At*SFC1 also transported succinate and fumarate to a lesser extent, but not malate, maleate, oxoglutarate, malonate, pyruvate, glutamate and aspartate. In addition, we confirmed by qRT-PCR that *At*SFC1 is highly expressed in young heterotrophic seedlings, flower, and young, mature and senescent leaves. Moreover, the lack of *At*SFC1 expression impacts germination, growth root and leaf metabolism.

MATERIAL AND METHODS

Plant material and growth conditions

All experiments were carried out using *A. thaliana* from the Columbia ecotype (Col-0). Seeds from wild-type and antisense lines were surface sterilized and imbibed for 2 days at 4 ℃ in the dark on 0.8% (*w*/*v*) agar plates

containing half-strength Murashige and Skoog (MS) medium, pH 5.7 (Murashige and Skoog, 1962). Seeds were subsequently germinated under short-day conditions (8h light/16h dark) in growth chamber at 150 µmol photons m^{-2} s^{-1} white light, 22 /20 ºC throughout the day/night cycle, and 60% relative humidity. After ten days under these conditions, the seedlings were transferred to a commercial substrate (Tropstrato HT®) and grown in growth chamber under the same conditions. Additionally, transgenic plants were generated with suppressed expression of *AtSCF1* gene by expressing antisense cDNA under the control of the *35S* promoter. Primers were designed (forward 5'- ATGGCGACGAGAACGGAATC-3' and reverse 5'-CTATAAAGGAGCATTCCGAAGATATCTCA-3') for the PCR amplification of full-length coding sequence of *At5g01340* gene from a cDNA library derived from Arabidopsis seedlings. The purified PCR fragment was cloned into pDONR207 vector using pDONR207 directional cloning kit (Thermo Fischer Scientific). The resultant ENTRY vector was used in the Gateway LR reaction (Thermo Fischer Scientific) with pH2WG7 Destination vector (Karimi et al., 2002) between the cauliflower mosaic virus 35S promoter and the t-nos terminator in the sense orientation and cloning of *SCF1* coding sequence in antisense orientation in the Expression vector. *Agrobacterium tumefaciens* GV3101 was transformed with the Expression vector and used for the transformation of *A. thaliana* ecotype Columbia-0 by floral dipping method (Clough and Bent, 1998). The antisense silencing construct for *AtSFC1* generate an amplicon of 930bp. To select transgenic plants, seeds were germinated on plates containing MS medium supplemented with 1% of sucrose and selective agent (*Hygromycin* 50 μL^{-1} L) in a growth chamber in the same conditions described above.

Genotype characterization

Total DNA was isolated from leaves. The antisense lines were checked by PCR analysis using specific primers for the resistance marker *Hygromycin* open reading frame, forward primer 5'-CGTGGTTGGCTTGTATGGAG-3' and reverse primer 5'-CCCAAGCTGCATCATCGAAA-3'. The PCR reactions were performed with Taq DNA polymerase (Invitrogen) according to manufacturer's

instructions, in a thermocycler programmed to perform an initial denaturation at 94 ℃ for 2 min, 35 cycles at 94 ℃ for 30 s; 58 ℃ for 15 s, 72 ° C for 45 s and a final extension of 72 ℃ for 5 min. The PCR products were a nalyzed in electrophoresis on 2% (w/v) agarose gel to confirm the mutant genotype.

Sequence analysis

The sequence of amino acids from ACR1 of *S. cerevisae* was used as a protein “query” sequence to search for protein homologues sequences using BLASTp (Basic Local Alignment Search Tool - protein) in the Nacional Center for Biotechnology Information (NCBI: htt://www.ncbi.nlm.nih.gov). The amino acid sequences were aligned with ClustaW multiple sequence alignment (htt://www.genome.jp/tools/clustaw) and GENEDOC software (Nicholas and Nicholas, 1997). The sequences of green plants showing the high similarity were selected for the alignment.

Expression analysis

After four weeks of growth leaf samples from wild type and antisense lines were collected and total RNA was extracted and purified using TRIzol® reagent (Invitrogen) according to manufacturer's recommendations. The integrity of the RNA was checked on 2% w/v agarose gels, and the concentration was measured before and after DNase I digestion using Gen5 Data Analysis Software (BioTek®). cDNA was synthesized from 2 µg total RNA using the Kit ImProm-II™ Reverse transcription system and oligo $dT_{(15)}$ primers (Promega, Brazil). PCR reactions were performed using an Applied Biosystem StepOne™ Real-Time PCR System and Power SYBR® Green qPCR Master Mix (Applied Biosystem). The amplification was performed using specific primers for *AtSFC1* cDNA forward primer 5’-TGAGATATCTTCGGAATGCTCC-3’ and reverse primer 5’-TCTTGATCAAATCAAAATCCTAACA-3’. To correct for differences in the amount of starting first-strand cDNAs, the actin gene (*ACT2* - At3g18780) *Arabidopsis* forward primer 5'-CTTGCACCAAGCAGCATGAA-3' and reverse primer 5'-CCGATCCAGACACTGTACTTCCTT-3' was amplified in parallel as

a reference gene. The specificity of PCR amplification was checked with the heat dissociation protocol following the final cycle of PCR. The relative quantification was performed according to the comparative method ($2^{-\Delta\Delta Ct}$), with the calibrator to various organs, ΔCt mature leaf ($\Delta\Delta Ct$ =0 and $2^{-\Delta\Delta Ct}$ = 1). For the remaining organs and seedling, the value of $2^{-\Delta\Delta Ct}$ indicates the fold change expression relative to calibrator. For the antisense lines $2^{-\Delta\Delta Ct} = 2^{\Delta Ct \text{ sample} - \Delta Ct \text{ calibrator}}$.

Bacterial expression of *AtSFC1*

The overproduction of *AtSFC1* as inclusion bodies in the cytosol of *E. coli* C0214 (DE3) was accomplished as described previously (Fiermonte et al., 1993; Picault et al., 2002). Control cultures with empty vector were processed in parallel. Inclusion bodies were purified on Sucrose density gradient, washed at 4 ºC with TE buffer (10mM Tris and 1mM EDTA, ph 7.0), then twice with a buffer containing Triton X-114 (3%, w/v), 1 mM EDTA, and 10 mM PIPES, pH 7.0, and once again with TE buffer. Protein was analyzed by SDS-PAGE on 17.5% gels; the identity of *At*SFC1 was confirmed by N-terminal sequencing and matrix-assisted laser desorption ionization-time of flight mass spectrometry of a trypsin digest of the purified protein excised from a Coomassie Brilliant Blue-stained gel. The yield of recombinant *At*SFC1 was estimated by laser densitometry as described previously (Fiermonte et al., 1998).

Reconstitution of the recombinant *At*SFC1 into proteoliposomes

Purified *At*SFC1 was solubilized in the presence of 1.45% sarkosyl (w/v), and a small residue was removed by centrifugation (258,000g for 30 min). Solubilized protein was diluted 6-fold with a buffer containing 20 mM Na2SO4 and 10 mM PIPES, pH 7.0, and then reconstituted by cyclic removal of detergent (Palmieri et al., 1995). The reconstitution mixture consisted of protein solution (75 mL, 0.09 mg), 10% Triton X-114 (75 mL), 10% phospholipids (egg lecithin from Fluka) as sonicated liposomes (100 mL), 10 mM ATP, AMP, or ADP (except where indicated otherwise), cardiolipin (0.6

mg; Sigma), 20 mM PIPES, pH 7.0, and water (final volume, 700 mL). The mixture was recycled 13 times through an Amberlite column (3.2 cm 3 0.5 cm) preequilibrated with buffer containing 20 mM PIPES, pH 7.0, and substrate at the same concentration as in the reconstitution mixture. All operations were performed at 4ºC, except for the passages through Amberlite, which were carried out at room temperature.

Transport measurements

External substrate was removed from the proteoliposomes on Sephadex G-75 columns preequilibrated with buffer A (50 mM NaCl and 10 mM PIPES, pH 7.0). Transport at 25 ºC was initiated by the addition of [^{14}C]Citrate (NEN Life Science Products) to the eluted proteoliposomes and terminated by the “inhibitor-stop” method (Palmieri et al., 1995). In controls, the inhibitors were added simultaneously to the labeled substrate. Finally, the external radioactivity was removed on Sephadex G-75 and radioactivity in the liposomes was measured (Palmieri et al., 1995). Transport activity was calculated by subtracting the control values from the experimental values. The initial rate of transport was calculated in millimoles per minute per gram of protein from the time course of isotope equilibration (Palmieri et al., 1995). Various other transport activities were assayed by the inhibitor-stop method. For efflux measurements, the internal substrate pool of the proteoliposomes was made radioactive by carrier-mediated exchange equilibration (Palmieri et al., 1995) with 0.1 mM [^{14}C] Citrate added at high specific radioactivity. After 60 min, residual external radioactivity was removed by passing the proteoliposomes again through a column of Sephadex G-75 eluted with buffer A. Efflux was started by adding unlabeled external substrate or buffer A alone and terminated by adding the inhibitors indicated above.

Physiological characterization

Germination tests were conducted in two different conditions: half-strength medium supplemented with 1% sucrose (w/v) and sucrose-free. The seeds were plated in plastic Petri dishes (90 x 15mm) and stratified at 4 ℃ in

the dark for 2 days, and then incubated at 22℃ in the photoperiod 16h light/ 8h dark. Each plate was divided into four fields, where 35 sterile seeds of each genotype were distributed with four biological replicates. The germinated seed count was made daily. Radicle emergence was used as a morphological marker for germination. The results were evaluated as a percentage of daily germinated seeds.

Root growth

Root growth was performed as described by Palmieri et al. (2008b) with minor modifications. They were germinated on plates vertically square (120x120mm) containing MS medium supplemented with 1% sucrose, 60 seeds in total per genotype. After germination plates were transferred to a growth chamber at 150 µmol photons m^{-2} s^{-1} , maximum temperature of 22 ºC and a minimum of 18℃, 60% relative humidity and photoperiod of 8 h light /16h dark. The first measurement was held already on the second day after germination.

Measurements of photosynthetic parameters

Gas exchange parameters were determined on fully expanded leaves from four weeks old plants simultaneously with chlorophyll *a* (Chl *a*) fluorescence measurements using an open-flow infrared gas exchange analyzer system (LI-6400XT; LI-COR Inc., Lincoln, NE) equipped with an integrated fluorescence chamber (LI-6400-40; LI-COR Inc.). Instantaneous gas exchange parameters were measured after 1 h illumination during the light period under 1000 µmol photons m^{-2} s^{-1}. The reference CO_2 concentration was set at 400 µmol CO_2 mol^{-1} air. All measurements were performed using the 2 cm^2 leaf chamber at 25 ℃, and the leaf- to-air vapor pressure deficit was kept at 1.3 to 2.0 kPa, while the blue light was set to 10% of the total irradiance to optimize stomatal aperture. The stomatal conductance (*gs*, mol H_2O m^{-2} s^{-1}), CO_2 assimilation rate (A, µmol CO_2 m^{-2} s^{-1}), the maximum quantum yield of PSII chemistry (F*v*/F*m*), electron transport rate (ETR, µmol m^{-2} s^{-1}) and dark respiration (µmol CO_2 m^{-2} s^{-1}) were calculated as described by Lima et al

(2002). Dark respiration (Rd) was measured using the same gas exchange system as described above after 1 h in the dark period.

Determination of metabolite levels

Whole rosettes of 5-week-old plants were harvested along the 8h light/16h dark cycle in the middle of light period. Rosettes were flash frozen in liquid nitrogen and stored at -80 ºC until further analyzes. Extraction was performed by rapid grinding of tissue in liquid nitrogen and immediate addition of an ethanol series as previously described (Gibon et al., 2004) The soluble fractions were used for quantification of sugars, amino acids, malate, fumarate and leaf pigments. While the precipitate was washed twice in 80% ethanol for later quantification of starch and protein. The levels of starch, sucrose, fructose, and glucose in leaf were determined exactly as described previously by Fernie et al. (2001). Protein and amino acids were determined as described by Gibon et al. (2004). Malate and fumarate were determined exactly as detailed by Nunes-Nesi et al. (2007).

Fruit and seeds analysis

For phenotyping reproductive tissues, the seedlings were transferred to commercial substrate and were kept in growth room at 22 ± 2 ℃, 60% relativ e humidity, irradiance of 150 µmol photons m^{-2} s^{-1}, with a photoperiod of 12 h light and 12 h dark to seed production. Siliques from wild-type and transgenic plants were collected and cleared with 0.2N NaOH and SDS (Sodium dodecyl sulfate) 1% solution to remove chlorophyll according to (Yoo et al., 2012). Cleared siliques were scored for length and number of seeds under a dissecting microscope (Stemi 2000-C, Zeizz). Seeds were dried in the vacuum for 48h prior to the determination of the 1000 seed weight. Six plants per genotype were used for the analysis and ten siliques were sampled from each plant.

Statistical analysis

The experiments were conducted in a completely randomized design. Data were evaluated by variance analysis and tested for significance differences using Student's *t* test. The term significant is used in the text only when the change in question has been confirmed to be significant ($P < 0.05$). All statistical analyses were performed using algorithms embedded into Microsoft Excel®.

RESULTS

Sequence analysis of *At*SFC1

The sequence of the amino acids from yeast *Sc*ACR1 was used to search for homologous plant sequences (http://blast.ncbi.nlm.nih.gov/Blast.cgi). As previously described (Catoni el al., 2003) this analysis revealed that Arabidopsis protein (NP_195754.1) show 36% of identical amino acids when compared with *Sc*ACR1 carrier from yeast (Figure 1). Database searches revealed more five proteins that showed substantial degree of identity to yeast ACR1. Tomato (XP_004249636.1), tobacco (XP_016494159.1) and cucumber (XP_004137702.1) shown 38%, potato (XP_006338979.1) and black cottonwood (XP_002322991.2) 37% of identical amino acids when compared with *Sc*ACR1 from yeast (Figure 1). These proteins share 81% to 84% identity to *At*SFC1.

The *At*SFC1 gene (At5g01340) encodes a protein of 309 amino acids with a calculated molecular mass of 34 kDa. The NCBI database indicates that the amino acids sequences of yeast ACR1 and the *At*SFC1 present the same protein structure and domains characteristics of all MCF family members (Palmieri, 1994), six transmembrane domains and the presence of a 3-fold repeated domain representing mitochondrial energy transfer signatures (METS), as show in the Figure 1. The six hydrophobic regions of *At*SFC1 amino acids sequence also were confirmed by alignment surface method

(DAS: http://www.sbc.su.se/~miklos/DAS/tmdas.cgi) in accordance with the typical structure of the members of the MCF. The six transmembrane domains and motif signatures are also present in the others five predicted succinate/fumarate carrier (Figure 1). Before the first predicted transmembrane domains, all proteins exhibited comparable short N-terminal extensions, with exception of *Cucumis sativus* that show a slightly higher extension

Expression analysis of *At*SFC1 in different organs

*At*SFC1 gene expression was found in all organs analyzed in this study with higher levels in five days imbibed seeds (Figure 2). Considerable expression is also observed in flower bud and four days imbibed seeds. The expression is considerable lower in mature leaf, senescent leaf, vein and flower (Figure 2). The expression in young leaf displayed the lower expression level. The results of expression of flower bud, flower and leaves are in close agreement with the expression data previously described (Catoni et al., 2003). In addition, *in silico* expression analysis suggest expression of AtSFC1 in various tissues and on different growth stages of plant, such as differentiation and expansion of petals, anthesis, mature pollen and seed germination and leaf senescence (Supplemental Figure 1). Similar results were observed by GUS-staining experiments previously described (Catoni et al., 2003).

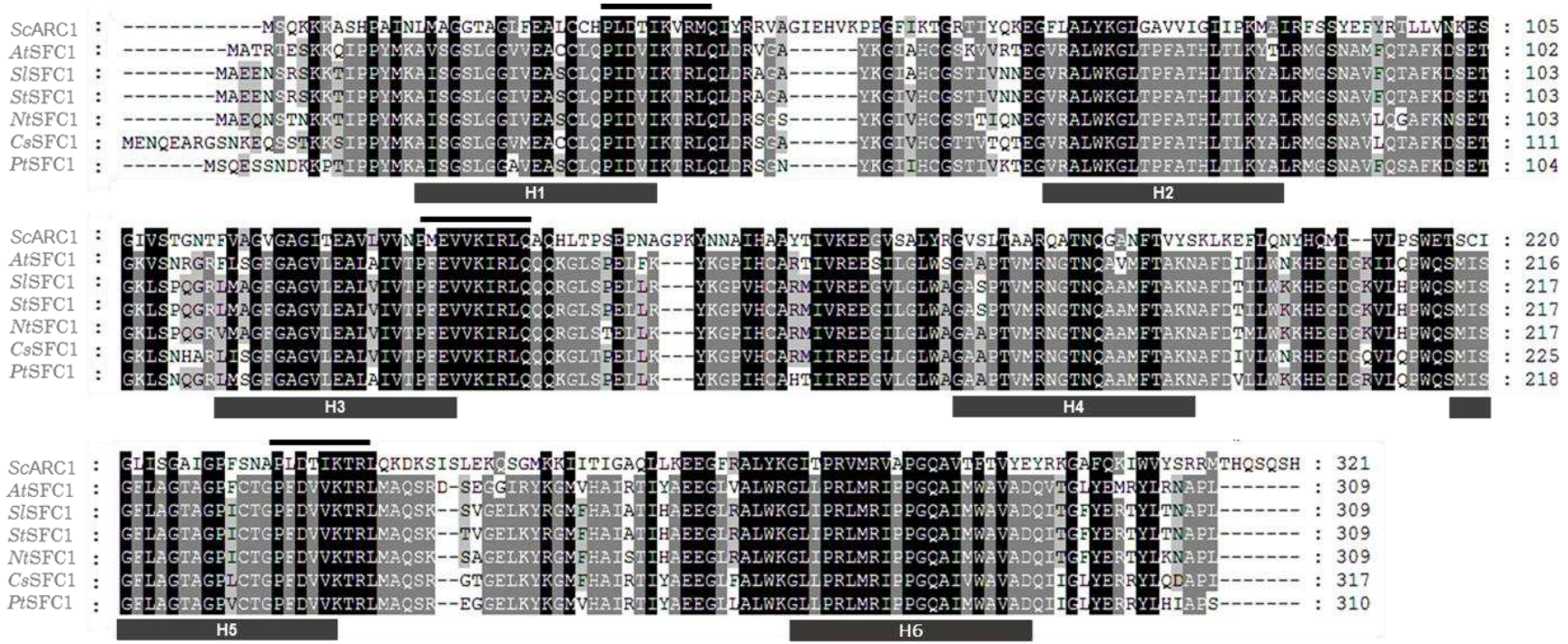

Figure 1. Alignment of the predicted amino acid sequence of *Sc*ACR1 with SFC1 homologues. The amino acids residues identical or similar among all family members are shaded in black and conserved residues are shaded in gray. Solid gray bars underline six putative membrane-spanning helices (H1-H6). Solid black bars above the sequences represents the conserved mitochondrial energy transfer signatures (P-x-[DE]-x-[LIVAT]-[RK]-x-[LRK]-[LIVMFY]-[QGAIVM]) characteristics of MCF proteins. The numbers indicates the amino acid positions. (*Sc*ACR1, succinate-fumarate carrier 1 from *Sacaromyces cerevisae*; *At*SFC1, succinate-fumarate carrier 1 from *Arabidopsis thaliana*; *Sl*SFC1 from *Solanum lycopersicum*; *St*SFC1, from *Solanum tuberosum; Nt*SFC1 from *Nicotiana tabacum*; *Cs*SFC1 from *Cucumis sativus*; *Pt*SFC1 from *Populus trichocarpa*). The sequence alignment was performed using the ClustalW (http://www.genome.jp/tools/clustalw).

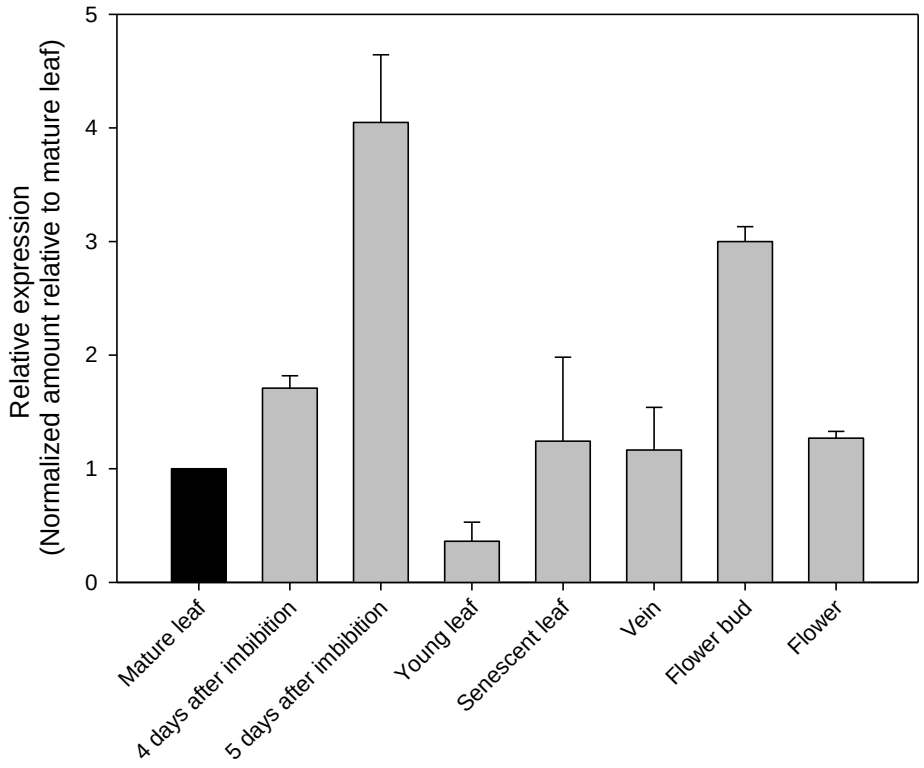

Figure 2. Expression of *At*SFC1 in seedling and some organs. Real-time PCR experiments were conducted on cDNAs prepared by RT of total RNAs from 4 and 5 days after imbibition and some organs, using gene specific primers to the *At*SFC1. Three independent preparations of total RNA (100ng) from each organ and stage of germination were assayed in triplicate. The relative quantification was performed according to the comparative method ($2^{-\Delta\Delta Ct}$). Actin2 was employed as a reference gene. For calibrator (*At*SFC1 mature leaf), $\Delta\Delta Ct = 0$ and $2^{-\Delta\Delta Ct} = 1$. For the remaining organs and seeds imbibed, the value of $2^{-\Delta\Delta Ct}$ indicates the fold change expression relative to calibrator. Values are means ± SE of three independent sampling.

Bacterial expression of *At*SFC1

The sequence of *At*SFC1 was overexpressed in *E. coli* C0214 (DE3) (Figure 3, lanes 2 and 4). It accumulated as inclusion bodies and was purified by centrifugation and washing (Figure 3, lane 5). The apparent molecular masses of the purified protein was about 35 kDa, in good agreement with the calculated value (34.1 kDa). The protein was not detected in bacteria

harvested immediately before the induction of expression (Figure 3, lanes 2 and 4), nor in cells harvested after induction but lacking the coding sequence in the expression vector. Approximately 11 mg of *At*SFC1 were obtained per liter of culture.

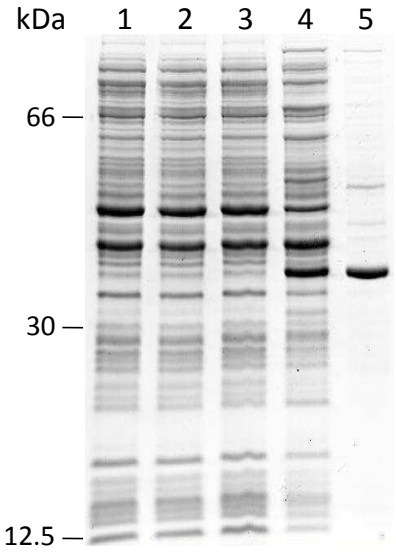

Figure 3. Expression in *E. coli* and purification of *At*SFC1**.** Proteins were separated by SDS-PAGE and stained with Coomassie Blue. Markers in left-hand column (bovine serum albumin, carbonic anhydrase and cytochrome c); lanes 1–4, *E. coli* C014 (DE3) containing the expression vector without (lanes 1 and 3) and with (lanes 2 and 4) the coding sequence of AtSFC. Samples were taken at the time of induction (lanes 1 and 2) and 4 h later at 37℃ (lanes 3 and 4). The same number of bacteria was analyzed in each sample. Lane 5, purified AtSFC1 protein (10 µg) derived from bacteria was shown in lane

Biochemical functional characterization of *At*SFC1

The recombinant *At*SFC1 protein was reconstituted into liposomes and its transport activities for a variety of potential substrates were tested in homoexchange experiments (i.e. with the same substrate inside and outside). Using internal and external substrate concentrations of 20 mM and 10 µM, respectively, the recombinant and reconstituted protein catalyzed an active ^{14}[C]-citrate/citrate exchange, which was completely inhibited by a mixture of bathophenanthroline and pyridoxal 5'-phosphate. They did not catalyze homoexchanges of malate, alpha-ketoglutarate, AMP, ADP, ATP (Figure 4). We were not able to test homo-exchange succinate transport because radiolabeled succinate was not available. Importantly, no ^{14}[C]-citrate/citrate exchange activity was detected if *At*SFC1 had been boiled before incorporation into liposomes or if proteoliposomes were reconstituted with sarkosyl-solubilized material from bacterial cells either lacking the expression vector for *At*SFC1 or harvested immediately before induction of expression. Likewise, no ^{14}[C]-citrate/citrate exchange activity was detected in liposomes reconstituted with two unrelated mitochondrial carriers encoded by the At5g48970 (thiamine diphosphate carrier) and SLC25A32 (solute carrier family 25, member 32) genes. The substrate specificity of *At*SFC1 was investigated in greater detail by measuring the uptake of ^{14}[C]-citrate into proteoliposomes that had been preloaded with a variety of potential substrates (Figure 4). The highest activity of ^{14}[C]-citrate uptake into proteoliposomes was with internal citrate, isocitrate, trans and cis-aconitate. ^{14}[C]-citrate also exchanged significantly, although to a lower extent, with internal fumarate, succinate and oxaloacetate. Notably, internal malate, maleate, oxoglutarate, malonate, pyruvate, glutamate and aspartate were not exchanged.

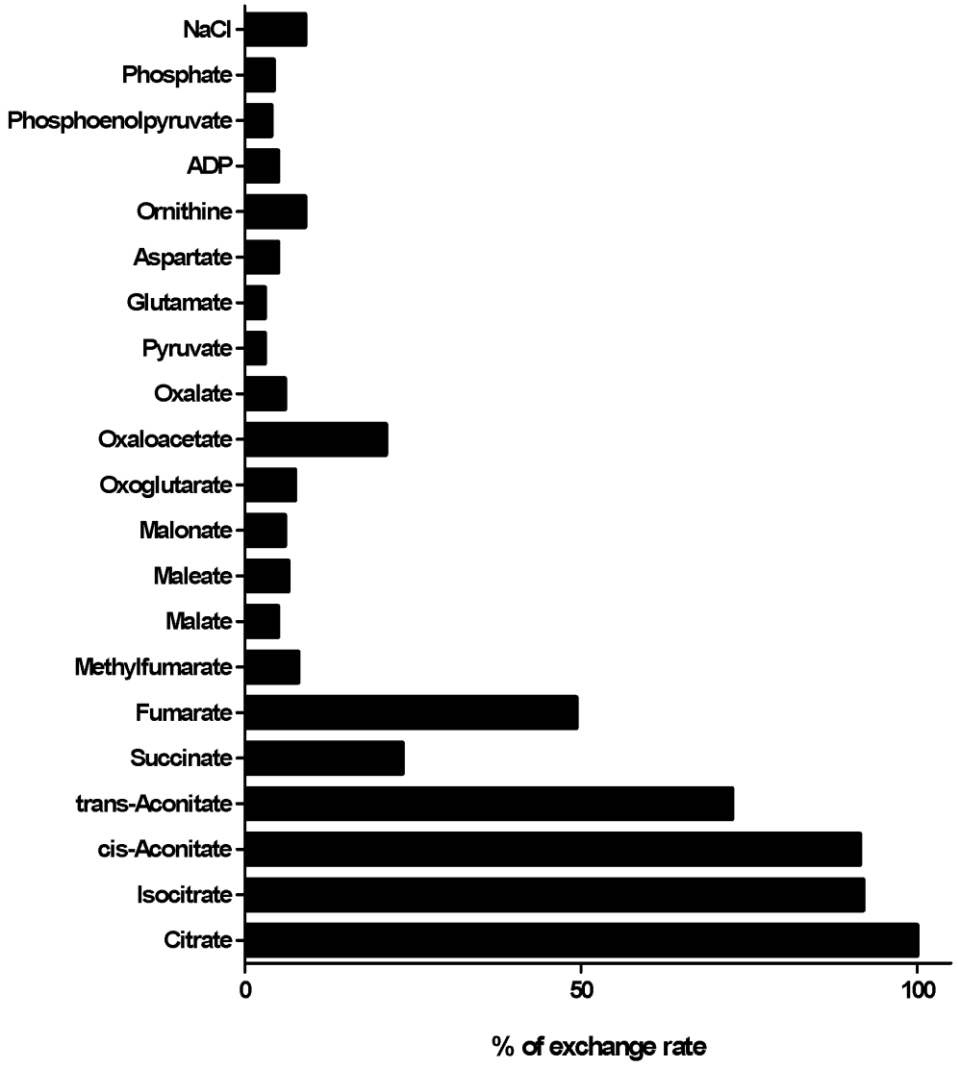

Figure 4. Dependence on internal substrate of the transport properties of liposomes reconstituted with recombinant *At*SFC1. Proteoliposomes were preloaded internally with various substrates (concentration, 10 mM). Transport was started by adding 0.13 mM ^{14}[C]-citrate after 1 min. The values are expressed as percentage of the ^{14}[C]-citrate/citrate exchange rate. Similar results were obtained in, at least, three independent experiments for each internal substrate investigated.

Kinetic characteristics of recombinant *At*SFC1

In Figure 5, the kinetics are compared for the uptake of 1 mM ^{14}[C]-citrate into reconstituted liposomes measured either as uniport (in the absence of internal citrate) or as exchange (in the presence of 10 mM citrate).

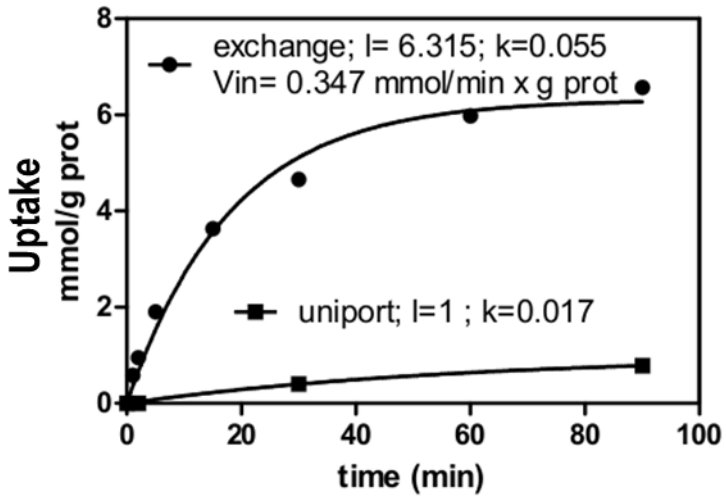

Figure 5. Kinetics of ^{14}[C]-citrate transport in proteoliposomes reconstituted with AtSFC. 1 mM ^{14}[C]-citrate was added to proteoliposomes containing 10 mM citrate (circles) or 5 mM NaCl and no substrate (squares).

The uptake of ^{14}[C]-citrate by exchange followed a first-order kinetics (rate constant 0.055 min^{-1}; initial rate 347 nmol / min per mg protein), isotopic equilibrium being approached exponentially. In contrast, the uniport uptake of citrate was very low. The uniport mode of transport by purified and reconstituted *At*SFC1 was further investigated by measuring the efflux of ^{14}[C]-citrate from prelabeled active proteoliposomes as it provides a more convenient assay for unidirectional transport. In the absence of external substrate little efflux was observed, nevertheless further analysis should be performed to confirm this result. However, upon addition of external citrate, cis-aconitate and importantly fumarate, an extensive efflux of radioactivity occurred and this efflux was prevented completely by the presence of the inhibitors pyridoxal 5'-phosphate and bathophenanthroline (Figure 6). Also the addition of succinate triggered a minor but significant ^{14}[C]-citrate efflux. These results indicate that, at least under the experimental conditions used, the reconstituted *At*SFC1 is able to catalyze a low uniport and a much faster exchange reaction of substrates.

The kinetic constants of recombinant *At*SFC1 were determined by

measuring the initial transport rate at various external ^{14}[C]-citrate concentrations, in the presence of a constant saturating internal concentration of 10 mM citrate. The transport affinity (Km) and the specific activity (Vmax) values for ^{14}[C]-citrate/citrate exchange at 25℃ were 0.13 ± 0.01 mM and 0.74 ± 0.14 mmol/min per g protein.

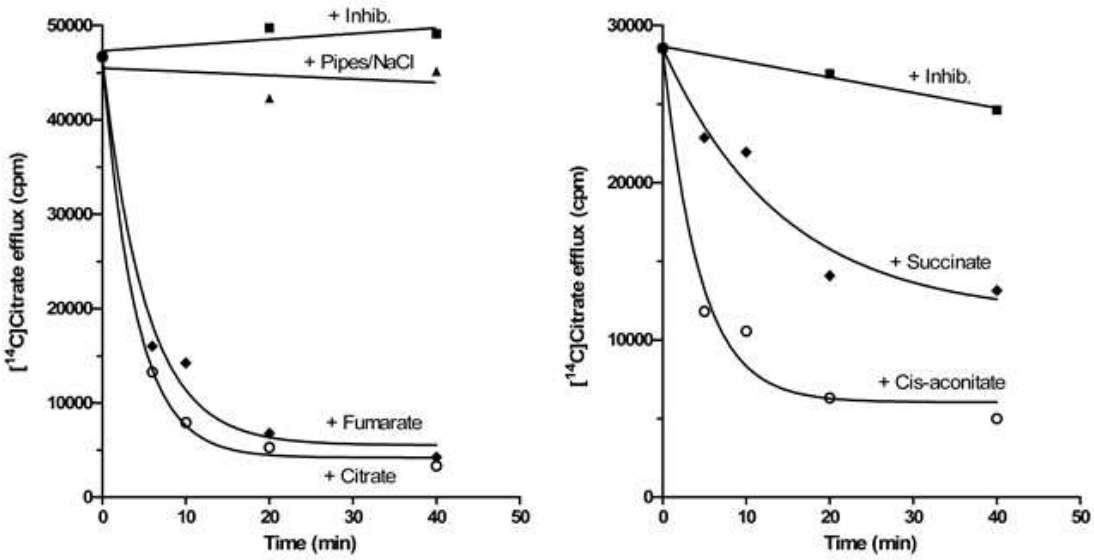

Figure 6. Efflux of ^{14}[C]-citrate from proteoliposomes. The internal substrate pool was labeled with ^{14}[C]-citrate by carrier-mediated exchange equilibration. Then the proteoliposomes were passed through Sephadex G-75. The efflux of ^{14}[C]-citrate was started by adding buffer A (Pipes 10mM, NaCl 50 mM, pH 7.0) alone , 5 mM citrate, 5 mM succinate, 5 mM fumarate, 5 mM cis-aconitate or 5 mM citrate plus 20 mM bathophenanthroline and 30 mM pyridoxal 5'-phosphate.

Generation and screening of 35S *At*SFC1 antisense lines

To understand the functional role of *At*SFC1 in plant metabolism we generated *Arabidopsis* 35S-*At*SFC1 antisense transgenic lines (Figure 7A). Firstly, the transgenic plants were selected on agar plates contained the selective agent (*Hygromicin)*. Posteriorly, leaves were harvested from the

resistant lines and checked by PCR analysis using specific primers for the resistance marker *Hygromycin.* Subsequently, RNA from the lines contained the resistant gene were extracted for expression analysis by a qRT-PCR strategy. In comparison with wild-type plants, eight lines showed reduced expression (Figure 7B). The lines *sfc1*-1, 2, 5, 6, 7, 8, and 10 showed 49%, 64%, 73%, 58%, 86%, 75%, 52% and 38% of the expression observed in wild-type, respectively. The line *sfc1*-12 the expression of the *At*SFC1 was lower than others lines, with 38% of the expression observed in wild-type. For the verify the probably effects of the reduction in the expression of *At*SFC1, we choosed only three lines with reduced expression of *At*SFC1 as followed, *sfc1*-8, *sfc1*-10 and *sfc1*-12.

Physiological characterization of *At*SFC1 antisense lines

Based on expression analysis (Figure 1 and Supplemental Figure 1) and in the predicted and the biochemical function of SFC1 (Figure 4) we decided to verify the importance of *At*SFC1 during seed germination. Thus, after the selection of the antisense lines, we confirmed the homozygosis of the transgenic lines and carried out measurements of seed germination rates (Figure 8). The seeds were germinated in half-strength MS medium in presence and absence of sucrose. With sucrose, the lines *sfc1*-12 and *sfc1*-8, showed low rate of germination 87% and 93%, respectively. However, the line 12 was significantly lower than wild type and the others lines (Figure 8A). By contrast, under sucrose-free, the line *sfc1*-10 showed the lower rate of germination with 83% (Figure 8B). Surprisingly, under these conditions, we did not observe any difference in seedling establishment between genotypes. However, seedlings that were grown in medium with sucrose, showed faster development when compared to sucrose-free medium.

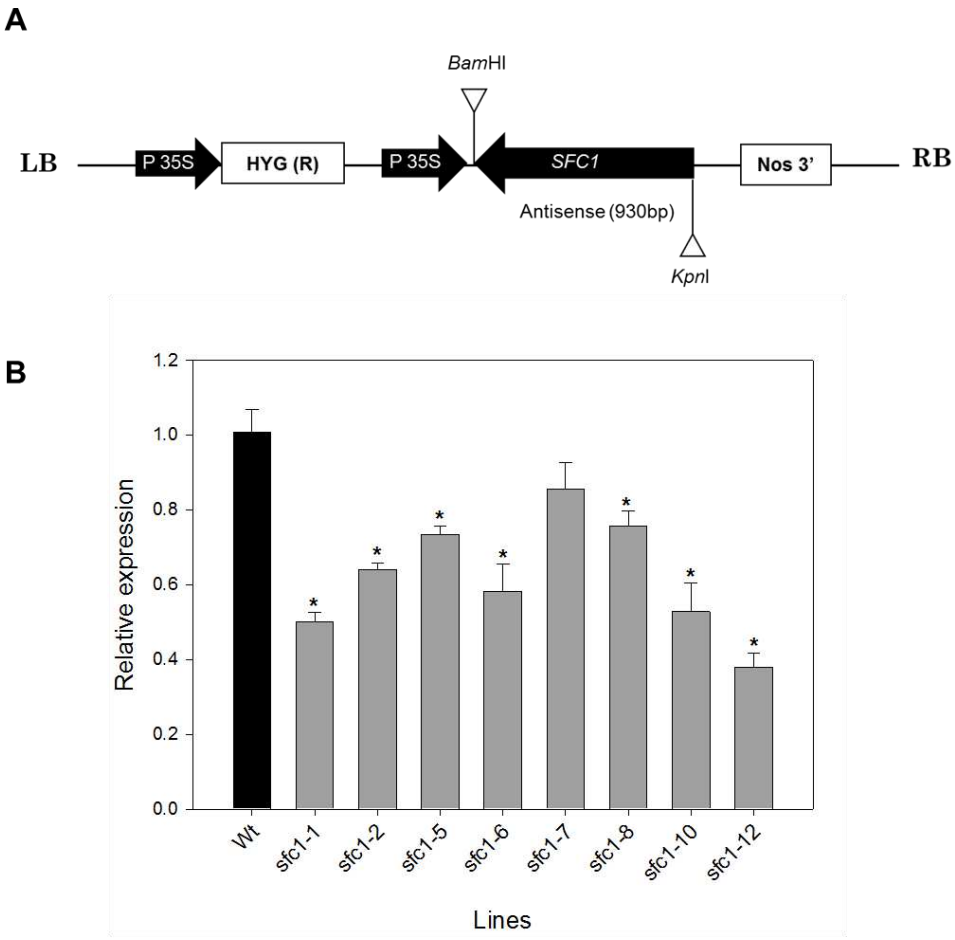

Figure 7. Expression analyses of silencing antisense construct to mitochondrial carrier *At*SFC1 in *Arabidopsis thaliana*. **(A)** A schematic representation of the antisense construct. A fragment of 930 bp of the gene *At*SFC1 was inserted in the antisense orientation under the control of the *35S* promoter. The cassette also contained a hygromycin resistance marker gene with *nos* promoter, and *nos* terminator. **(B)** Expression analyses of the *AtSFC1* in leaves of wild-type and antisense lines. Real-time PCR experiments were conducted on cDNAs prepared by RT of total RNAs from leaves, using gene specific primers to the *At*SFC1. Three independent preparations of total RNA (100ng) were assayed in triplicate. The relative quantification was performed according to the comparative method ($2^{-\Delta\Delta Ct}$). Actin2 was employed as a reference gene. The levels of transcripts of the antisense lines were normalized to the levels of transcripts of wild-type, $\Delta\Delta Ct = 0$ and $2^{-\Delta\Delta Ct} = 1$. Values are means ± SE of three independent sampling; an asterisk indicates values that were determined by the Studen's *t*-test to be significabtly different ($P < 0.05$) from the wild-type.

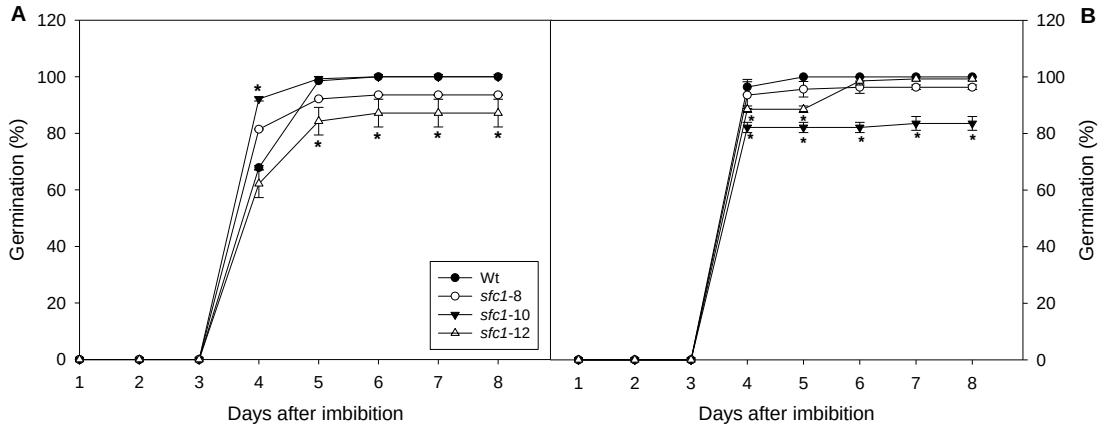

Figure 8. Germination rate of antisense lines to *AtSFC1* gene. (A) 0.5 MS medium supplemented with sucrose. (B) half-strength MS medium sucrose-free. Radicle emergence was used as a morphological marker for germination. At least 35 seeds per genotype were measured in each replicate. The seeds were stratified at 4 ℃ in the dark for 2 days and then incubated at 22℃ in the photoperiod 16h light/ 8h dark. Standard errors are based on four biological replicates. The asterisk indicates values that were determined by Student's *t*-test to be significantly different ($P < 0.05$) from wild-type.

In silico analysis as well as GUS-staining activity (Catoni et al., 2003), indicated that *At*SFC1 is also expressed in roots. To further investigate the physiological role of *At*SFC1 in roots, we analyzed root growth in the antisense lines. For this, we germinated seed on vertical agar plates and recorded root length (Supplemental Figure 2). Interestingly the roots from all transgenic lines were shorter than those of wild-type plants (Figure 9). Nevertheless, after 6 days of germination, the root length of the line *sfc1*-8 was quite similar than wild-type.

Additionally, we grew all transgenic plants side by side with wild type plants on soil and evaluated the gas exchange, chlorophyll *a* fluorescence and growth parameters. The CO_2 assimilation rate was significantly higher than that observed in the wild-type control in all antisense lines (Figure 10A). Likewise, there was a clear tendency of increase in stomatal conductance, which was significantly higher than wild-type in the *sfc1*-12 line (Figure 10B). Furthermore, the antisense lines to *At*SFC1 displayed unaltered F_v/F_m and

ETR (Figure 10C and D, respectively). However, although no significant difference, the electron transport rate, respiration rate (Figure 10E) and transpiration (Figure 10F) in the antisense lines were slightly higher than wild type. We did not observed differences in root and shoot dry weight between the antisense lines and wild type (Supplemental Figure 3).

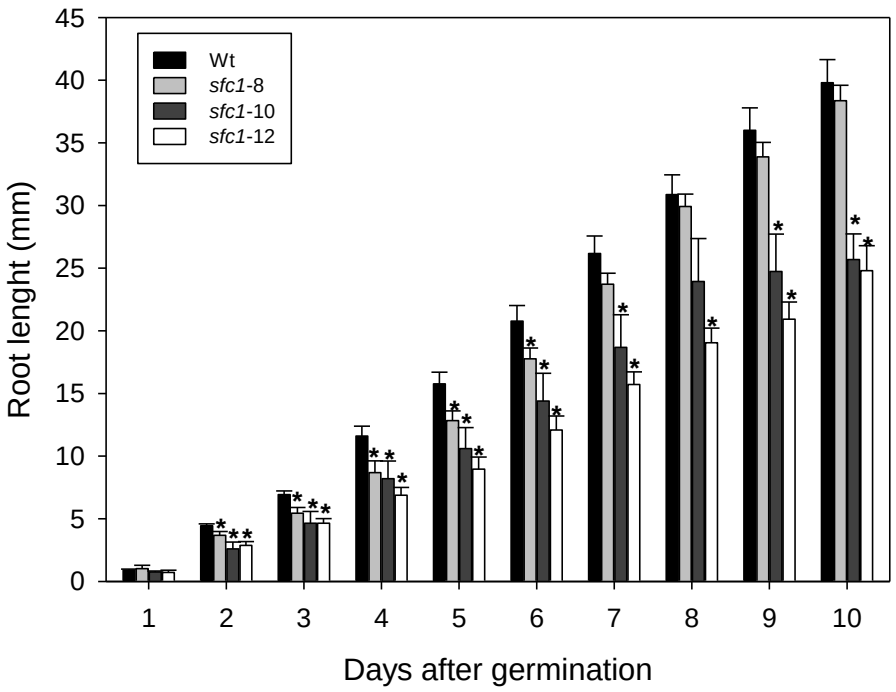

Figure 9. Root length of the wild-type (Wt) and antisense lines to *AtSFC1* plants at 11 days after germination. Ten seeds per genotype were germinated on vertical plates for 2 days in the dark and then transferred to 8h light/16h dark regime. Values are means ± SE of ten measurements from six biological replicates; an asterisk indicates values that were determined by the Student's *t*-test to be significantly different ($P < 0.05$) from the wild-type.

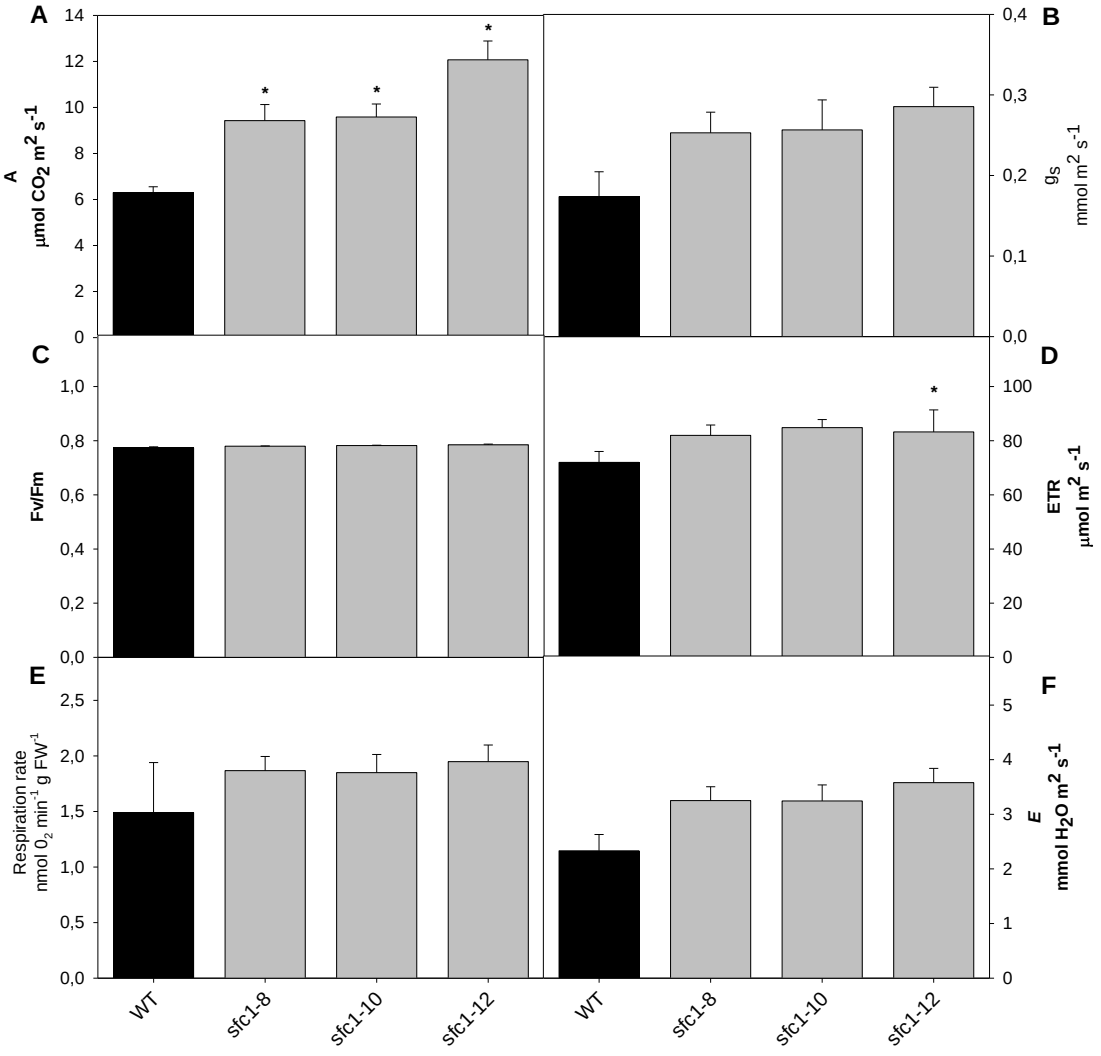

Figure 10. Effect of the decreased of the expression of *AtSFC1* on the gas exchange and fluorescence parameters. **(A)** leaf assimilation rate as a function of light intensity, **(B)** stomatal conductance (g_s) as a function of light intensity, , **(C)** the maximum quantum yield of PSII, **(D)** electron transport rate of photosystem 2 (PSII) **(E)** dark respiration measurements, **(F)** transpiration rate as a function of light intensity. All measurements were performed in 4- to 5-weeks-old plants. All parameters were measured by Infrared gas analyzer (IRGA). Values are means ± SE of six individual determinations per line. An asterisk indicates values that were determined by the Student's *t*-test to be significantly different ($P < 0.05$) from the wild-type.

We also measured in leaves the levels of metabolites involved with carbon and nitrogen metabolism (Figure 11). No differences were observed in the levels of glucose and sucrose (Figure 11A e C, respectively). Differently, the levels of fructose were significantly higher in the line *sfc1*-12 (Figure 11B). Higher levels of starch were also observed in transgenic lines (Figure 11D). Minor changes were observed in the levels of malate and fumarate, which were significantly higher only in the line *sfc1*-8. Concerning the main nitrogen containing compounds higher levels of total protein and amino acids were observed in leaves of all analyzed transgenic lines in comparison with the wild type control (Figure 11G and H, respectively). However, no differences were observed in terms of photosynthetic pigments (Supplemental Figure 4).

Concerning silique production it was observed that the number of silique produced per plant was not consistently affected in the antisense lines (Figure 12). The lines *sfc1*-12 showed a reduced number of siliques, whereas *sfc1*-10 showed reduced number of siliques per plant, however, this value was significant lower than wild-type. In contrast, the *sfc1*-8 line displayed high number of siliques per plant (Figure 12A). In agreement with higher CO_2 assimilation rate observed in the transgenic lines, the silique length was higher than wild type in all antisense lines, being significantly higher in the lines *sfc1*-10 and *sfc1*-12 (Figure 12B). Similar observation was made for the number of seeds per silique, which was higher in all transgenic lines (Figure 12C). On the other hand, any difference was observed in terms of weight of 1000 seeds, except for *sfc1*-8 that was a lower than the wild type control (Figure 12D).

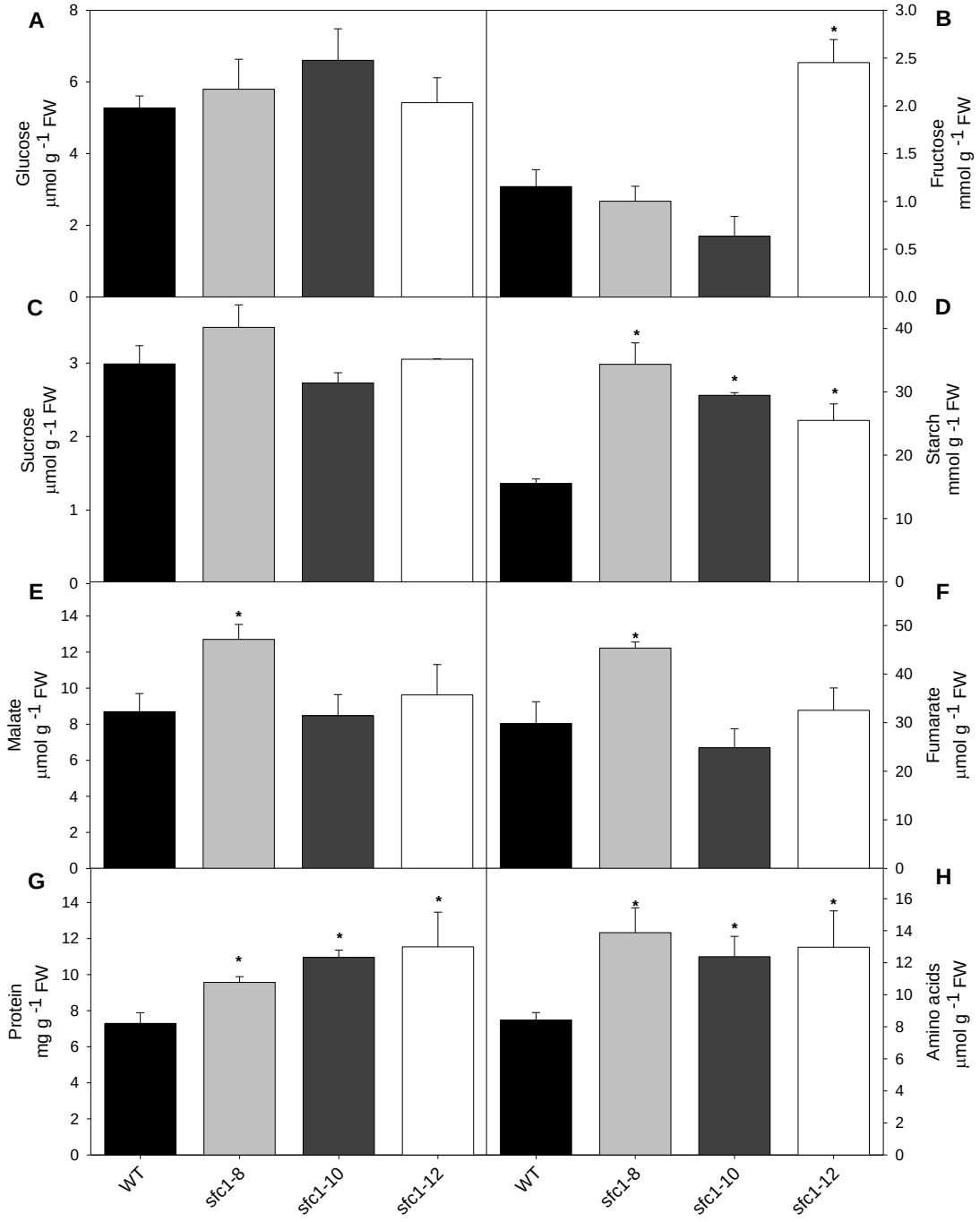

Figure 11. Changes in the metabolites content in leaves of antisense lines *At*SFC1. **(A)** Glucose, **(B)** Fructose, **(C)** Sucrose, **(D)** Starch, **(E)** Malate, **(F)** Fumarate, **(G)** Protein an **(H)** Amino acids. Samples were taken from mature source leaves. Values are means ± SE of six individual determinations per line. An asterisk indicates values that were determined by the Student's *t*-test to be significantly different ($P < 0.05$) from the wild-type. FW: fresh weight.

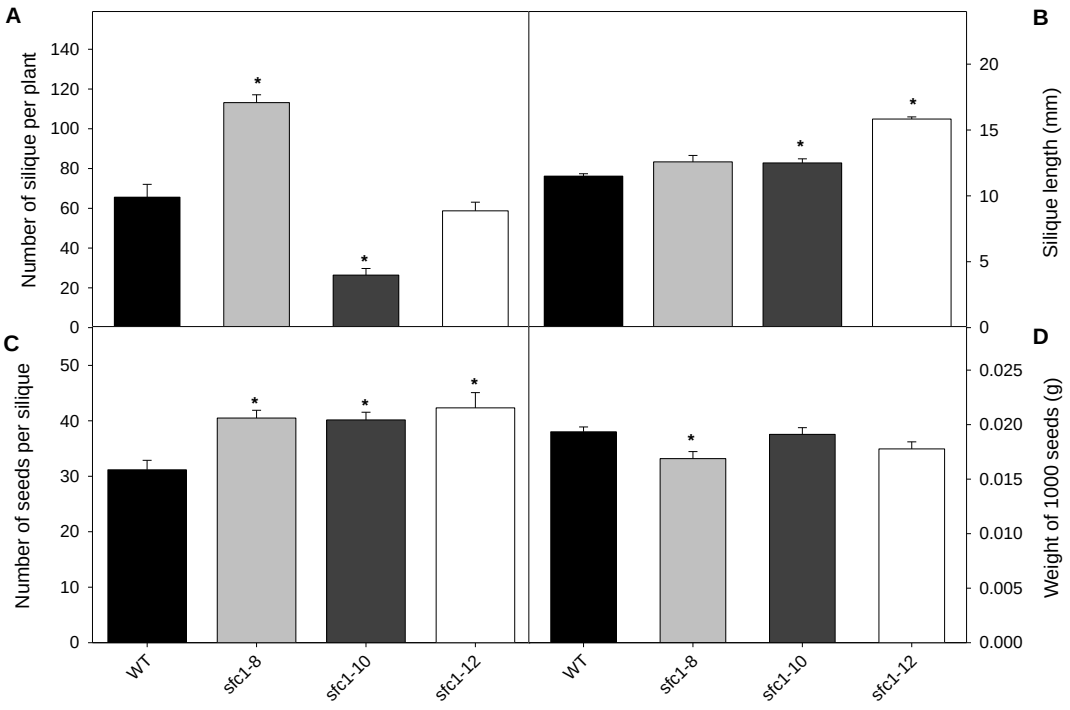

Figure 12. Seed yield parameters. **(A)** number of silique per plant, **(B)** silique length, **(C)** number of seeds per silique, **(D)** weight of 1000 seeds in grams. Values are means ± SE of six individual determinations per line. An asterisk indicates values that were determined by the Student's *t*-test to be significantly different ($P < 0.05$) from the wild-type.

DISCUSSION

The information on the correct subcellular localization is indispensable to understand the role of a protein in metabolism (Kirchberger et al., 2008; Bahaji et al., 2011). In this context, mitochondrial complexome profiling datasets reveal that the *At*SFC1 protein is localized in the inner membrane mitochondria (Braun et al., 2016 unpublished). In addition, it has been shown that *At*SFC1 protein have the typical structure of a MCF protein (Catoni et al., 2003) as well as the homologues predicted proteins analyzed in this study due the presence of the 3-fold repeated signature motif (Figure 1) that is typical

feature of transports proteins belonging to the MCF family (Millar and Heazlewood, 2003).

Interestingly, the results presented in this work provide evidence that *At*SFC1 upon reconstitution into liposomes, a powerful tool to identify the functional properties of a gene (Borecky et al., 2001; Scalise et al., 2013), showed a high substrate specificity, for citrate and isocitrate, and to a lesser extent, fumarate and succinate (Figure 4). Thus, *At*SFC1 differs from the well-known yeast ACR1 carrier (Palmieri et al., 1997) due the main substrate affinity and mechanism of transport. The ACR1 carrier transport very low extent citrate and isocitrate and catalyze only a counter-exchange transport. In contrast, the *At*SFC1 transport preferentially citrate and isocitrate in an antiport or uniport system.

Concerning the physiological role in plant metabolism it is conceivable that the reduced expression of *At*SFC1 seems to have minor impact on seed germination (Figure 8). During the germination of *Arabidopsis*, the fatty acids are broken down and converted to sucrose and some respired (Eastmond et al., 2000; Eastmond and Graham, 2001; Pracharoenwattana et al., 2005). Research about germination using lettuce and sunflower seeds suggest that fatty acids can be respired during germination, before the development of a fully functional glyoxylate cycle (Salon et al., 1988; Raymond et al., 1992). In addition, experiments using *Arabidopsis* mutant lacking ICL (isocitrate lyase) exhibited reduced growth and lipid mobilization only under suboptimal growing conditions (Eastmond et al., 2000) and lipid catabolism in the *Arabidopsis* mutant lacking MLS (malate synthase) appeared unaffected (Cornah et al., 2004). By contrast, the lack of peroxisomal CSY (citrate synthase) activity inhibited lipid catabolism and prevented seedling establishment (Pracharoenwattana et al., 2007). These findings together suggest the obligatory export of citrate from peroxisomes into the cytosol, which could enter in the mitochondria through specifics transporters. Nevertheless, it is unclear that *At*SFC1 to be related with the glyoxylate cycle. For this, will be necessary, germinate seeds in the dark, once that the glyoxylate cycle mutants are more severely affected under these conditions.

Additionally, the seedlings with reduced expression of *At*SFC1 displayed a reduced root growth (Figure 9). These results suggest a restricted

rate of root respiration and a lower energy production in the roots impairing growth. Thus we believe that citrate from the beta oxidation is not efficiently imported by the mitochondria in the roots.

Interestingly the transgenic lines showed an elevated photosynthetic rate (Figure 10A), which was accompanied by a high stomatal conductance (Figure 10D) with minor and not significant changes in electron transport rates (Figure 10B). The increase in photosynthesis did not resulted in changes biomass accumulation (Supplemental Figure 3), but with increase in silique length and seed number (Figure 12). Taken together, despite the fact that these results and those obtained in previous study (Catoni et al., 2003) showed that *At*SFC1 has a reduced expression in autotrophic tissues, our results indicates that the reduction in its expression lead to higher stomatal conductance and CO_2 assimilation rate. It has been shown that mitochondrial metabolism plays important roles in optimizing photosynthesis (Noctor et al., 2003). This communication can be influenced at the enzyme level. Illuminated leaves with lower expression and activity of ACO and the mitochondrial MDH showed enhanced photosynthetic rates (Carrari et al., 2003; Nunes-Nesi et al., 2005). In contrast, inhibition of citrate synthase or isocitrate dehydrogenase have no effect on the rates of photosynthesis (Sienkiewicz-Porzucek et al., 2008; 2010; Sulpice et al., 2010). On the other hand, from our results the increase of photosynthesis in the transgenic lines can be associated with stomatal aperture. It is well known that the efflux of malate from guard cells can regulate the activity of anion channels on guard cell membrane (Lee et al., 2008; Kim et al., 2010). Thus, the content of organic acids can modulate the functioning of guard cells and, in turn, affect the stomatal movements. In this sense, it seems plausible that an impaired citrate transport can probably culminates an alteration in stomatal movements that directly or indirectly can be associated with enhancement of photosynthesis. Nevertheless, the mechanisms involved should be further investigated.

The reduction in the expression of *At*SFC1 lead to remarkable increase in starch levels (Figure 11D), without changes in sucrose contents (Figure 11C). Cumulative evidence, has shown that alterations in the metabolism of organic acids in mitochondria can lead to changes in redox state of plastids (Michalska et al., 2009). In tomato plants with reduced expression of

mitochondrial malate dehydrogenase isoform in fruits it was shown that, changes in malate metabolism in mitochondria affect starch biosynthesis in the amyloplast (Centeno et al., 2011). This alteration is related to changes in redox status of the chloroplast, which would change the activation state of ADP-glucose pyrophosphorylase (AGPase) (Centeno et al., 2011). Although it has not yet been experimentally demonstrated the direct involvement of citrate in the regulation of starch synthesis, we can speculate that the impaired of *At*SFC1 causes changes in the transport of citrate and isocitrate, leading to changes in the levels of organic acids in mitochondria and consequently implying in the activation of AGPase. Therefore, further analysis are required to check whether the reduced expression of the *At*SFC1 influence in the activation of AGPase in amyloplasts due an alterations in the contents of organic acids in the mitochondria. We can also explain that the larger proportion of the fixed carbon observed in lines is retained as starch in the leaf. Interestingly, this accumulation did not reflect the increase in biomass (Supplemental Figure 3). In conditions where the supply of carbon exceeds its use for growth, starch is not completely degraded during the night which results in a progressive increase in starch content from day to day (Pilkington et al., 2015).

Additionally, it was shown that *At*SFC1 is related to the levels of protein and amino acids (Figure 11G and H, respectively). The hypothesis that cytosolic isocitrate dehydrogenase (ICDH) plays an important role in the production of carbon skeletons for NH_4^+ assimilation has recently been supported indirectly by some observations. Sulpice et al. (2010) showed that plants deficient in the cytosolic ICDH presented alterations in the activities of enzymes involved in primary nitrate assimilation and in the synthesis of 2-oxoglutarate leading in decrease of total amino acids levels. In this context, considering as an important metabolic branch point, citrate and isocitrate conversions may provide carbon skeletons for nitrogen assimilation and reducing equivalents for biosynthetic reactions (Popova and Pinheiro de Carvalho, 1998). One explanation could be that the citrate is isomerized into isocitrate and then oxidize by NADP-dependent isocitrate dehydrogenase (ICDH) generating 2-oxoglutarate. The latter, can be exported to the plastids, where it can be used in nitrogen metabolism (Hodges, 2002). Thus,

biochemical studies needs to be carried out for to define the exact mechanism underlying this phenomenon.

Another striking effect was an increase of number of seeds per silique (Figure 12C). The expression of the *At*SFC1 is high in the reproductive tissues. In this sense, it was expected that the number of seeds per silique was reduced. In addition, the lines showed high CO_2 assimilation followed by an increase of starch and amino acids levels. Taken together, our results suggest that, these skeletons of carbon are channeled to reproductive organs as source of carbon for biosynthetic pathways and energy production. These compounds, mainly amino acids, plays an important role in organic nitrogen allocation in developing siliques (Ladwig et al., 2012). Histochemical analysis of Arabidopsis amino acid transporters - 8 (AAP8) revealed stage-dependent expression in siliques and developing seeds. Thus, AAP8 is probably responsible for import of organic nitrogen into developing seeds (Okumoto et al., 2002).

Given the transport characteristics added to the effects in the metabolism, we hypothesize that the primary function of the *At*SFC1 is probably to catalyze the exchange between cytosolic citrate and intramitochondrial isocitrate. The partitioning of citrate between the glyoxylate cycle, beta-oxidation fatty acids and respiratory pathway may be determined by the relative demands for sugar or energy by seedling (Pracharoenwattana et al., 2005). It is seems reasonable to assume the transport of the citrate and isocitrate in the opposite direction too, catalyzing the exchange between cytosolic isocitrate and intramitochondrial citrate. The latter is known to be stored in the vacuole during the night and broken down during the day primarily as a source of carbon for nitrogen assimilation (Cheung et al., 2014). Perhaps the transporter is involved in partitioning citrate between the mitochondria and cytosol.

CONCLUSIONS

The experiments described in this study strongly suggest that *At*SFC1 is a transporter protein in the mitochondrial inner membrane of *Arabidopsis*. From its transport properties and kinetic parameters, *At*SFC1 transport mainly tricarboxylates (citrate, isocitrate, *cis*-aconitate and *trans*-aconitate) and, less efficiently dicarboxylates such as succinate and fumarate. This transport seems to connects the anaplerotic production of citrate by the glyoxylate cycle in the peroxisome with the TCA cycle in the mitochondria. The cytoplasmic isocitrate can enter in the peroxisome and participate of the glyoxylate cycle reactions supporting the gluconeogenesis. On the other hand, it can be oxidized by isocitrate dehydrogenase generating 2-oxoglutarate, which can be used as a carbon skeleton for amino acids biosynthesis or an intermediate of TCA cycle. In addition, this carrier seems be important during reserves mobilization of the oilseeds and support of respiration, once that the early of stages of germination was compromised as well as the root growth. Finally, in autotrophic tissues such as leaves, *At*SFC1 seems to be involved in the optimization of photosynthesis leading a consequent increase in starch and amino acids levels in mature leaves. However, further analysis are still necessary to elucidate the involved mechanisms.

REFERENCES

Bahaji A, Muñoz FJ, Ovecka M, Baroja-Fernández E, Montero M, Li J, Hidalgo M, Almagro G, Sesma MT, Ezquer I, et al (2011) Specific delivery of AtBT1 to mitochondria complements the aberrant growth and sterility phenotype of homozygous Atbt1 Arabidopsis mutants. Plant J **68**: 1115–1121

Borecky J, Maia IG, Costa AD, Jezek P, Chaimovich H, Andrade PBM, Vercesi AE, Arruda P (2001) Functional reconstitution of Arabidopsis thaliana plant mitochondrial uncoupling protein (AtPUMP1) expressed in Escherichia coli. FEBS Lett **505**: 240–244

Carrari F, Nunes-Nesi A, Gibon Y, Lytovchenko A, Loureiro ME, Fernie AR (2003) Reduced expression of aconitase results in an enhanced rate of photosynthesis and marked shifts in carbon partitioning in illuminated leaves of wild species tomato. Plant Physiol **133**: 1322–35

Catoni E, Schwab R, Hilpert M, Desimone M, Schwacke R, Flügge UI, Schumacher K, Frommer WB (2003) Identification of an Arabidopsis mitochondrial succinate-fumarate translocator. FEBS Lett **534**: 87–92

Centeno DC, Osorio S, Nunes-Nesi A, Bertolo ALF, Carneiro RT, Araújo WL, Steinhauser M-C, Michalska J, Rohrmann J, Geigenberger P, et al (2011) Malate plays a crucial role in starch metabolism, ripening, and soluble solid content of tomato fruit and affects postharvest softening. Plant Cell **23**: 162–84

Cheung CYM, Poolman MG, Fell DA, Ratcliffe RG, Sweetlove LJ (2014) A Diel Flux Balance Model Captures Interactions between Light and Dark Metabolism during Day-Night Cycles in C3 and Crassulacean Acid Metabolism Leaves. Plant Physiol **165**: 917–929

Clough SJ, Bent AF (1998) Floral dip: a simplified method for Agrobacterium-mediated transformation of Arabidopsis thaliana. Plant J **16**: 735–43

Cornah JE, Germain V, Ward JL, Beale MH, Smith SM (2004) Lipid utilization, gluconeogenesis, and seedling growth in Arabidopsis mutants lacking the glyoxylate cycle enzyme malate synthase. J Biol Chem **279**: 42916–42923

Eastmond PJ, Germain V, Lange PR, Bryce JH, Smith SM, Graham IA (2000) Postgerminative growth and lipid catabolism in oilseeds lacking the glyoxylate cycle. Proc Natl Acad Sci U S A **97**: 5669–5674

Eastmond PJ, Graham IA (2001) Re-examining the role of the glyoxylate cycle in oilseeds. Trends Plant Sci **6**: 72–77

Farre EM, Tiessen A, Roessner U, Geigenberger P, Trethewey RN (2001) Analysis of the Compartmentation of Glycolytic Intermediates , Nucleotides , Sugars , Organic Acids , Amino Acids , and Sugar Alcohols in Potato Tubers Using a Nonaqueous Fractionation Method 1. **127**: 685–700

Fernie AR, Roessner U, Geigenberger P (2001) The sucrose analog palatinose leads to a stimulation of sucrose degradation and starch synthesis when supplied to discs of growing potato tubers. Plant Physiol **125**: 1967–77

Fiermonte G, Dolce V, Palmieri F (1998) Expression in Escherichia coli, functional characterization, and tissue distribution of isoforms A and B of the phosphate carrier from bovine mitochondria. J Biol Chem **273**: 22782–7

Fiermonte G, Walker JE, Palmieri F (1993) Abundant bacterial expression and reconstitution of an intrinsic membrane-transport protein from bovine mitochondria. Biochem J **294**: 293–299

Godavari HR, Badour SS, Waygood ER (1973) Isocitrate lyase in green leaves. Plant Physiol **51**: 863–7

Graham IA (2008) Seed Storage Oil Mobilization. Annu Rev Plant Biol **59**: 115–142

Hodges M (2002) Enzyme redundancy and the importance of 2-oxoglutarate in plant ammonium assimilation. J Exp Bot **53**: 905–916

Hunt L, Fletcher J (1977) Intracellular location of isocitrate lyase in leaf tissue. Plant Sci Lett **10**: 243–247

Karimi M, Inzé D, Depicker A (2002) GATEWAY^{TM} vectors for Agrobacterium-mediated plant transformation. Trends Plant Sci **7**: 193–195

Kim T-H, Ohmer M, Hu H, Nishimura N, Schroeder JI (2010) Guard Cell Signal Transduction Network: Advances in Understanding Abscisic Acid,

CO 2 , and Ca 2+ Signaling. Annu Rev Plant Biol **61**: 561–91

Kirchberger S, Tjaden J, Ekkehard Neuhaus H (2008) Characterization of the Arabidopsis Brittle1 transport protein and impact of reduced activity on plant metabolism. Plant J **56**: 51–63

Klingenberg M (2008) The ADP and ATP transport in mitochondria and its carrier. Biochim Biophys Acta - Biomembr **1778**: 1978–2021

Krueger S, Giavalisco P, Krall L, Steinhauser MC, B??ssis D, Usadel B, Fl??gge UI, Fernie AR, Willmitzer L, Steinhauser D (2011) A topological map of the compartmentalized Arabidopsis thaliana leaf metabolome. PLoS One. doi: 10.1371/journal.pone.0017806

Kunze M, Pracharoenwattana I, Smith SM, Hartig A (2006) A central role for the peroxisomal membrane in glyoxylate cycle function. Biochim Biophys Acta - Mol Cell Res **1763**: 1441–1452

Ladwig F, Stahl M, Ludewig U, Hirner AA, Hammes UZ, Stadler R, Harter K, Koch W (2012) Siliques are Red1 from Arabidopsis acts as a bidirectional amino acid transporter that is crucial for the amino acid homeostasis of siliques. Plant Physiol **158**: 1643–1655

Lee M, Choi Y, Burla B, Kim Y-Y, Jeon B, Maeshima M, Yoo J-Y, Martinoia E, Lee Y (2008) The ABC transporter AtABCB14 is a malate importer and modulates stomatal response to CO2. Nat Cell Biol **10**: 1217–1223

Lima ALS, DaMatta FM, Pinheiro HA, Totola MR, Loureiro ME (2002) Photochemical responses and oxidative stress in two clones of Coffea canephora under water deficit conditions. Environ Exp Bot **47**: 239–247

Linka N, Weber APM (2010) Intracellular metabolite transporters in plants. Mol Plant **3**: 21–53

Lunn JE (2007) Compartmentation in plant metabolism. J Exp Bot **58**: 35–47

Michalska J, Zauber H, Buchanan BB, Cejudo FJ, Geigenberger P (2009) NTRC links built-in thioredoxin to light and sucrose in regulating starch synthesis in chloroplasts and amyloplasts. Proc Natl Acad Sci U S A **106**: 9908–13

Millar AH, Heazlewood JL (2003) Genomic and proteomic analysis of mitochondrial carrier proteins in Arabidopsis. Plant Physiol **131**: 443–53

Murashige T, Skoog F (1962) A Revised Medium for Rapid Growth and Bio Assays with Tobacco Tissue Cultures. Physiol Plant **15**: 473–497

Nicholas KB, Nicholas HBJr (1997) Genedoc: a tool for editing and annotating multiple sequence alignments. Embnew news **4:**14

Noctor G, Dutilleul C, Paepe R De, Foyer CH (2003) Use of mitochondrial electron transport mutants to evaluate the effects of redox state on photosynthesis, stress tolerance and the integration of carbon/nitrogen metabolism. J Exp Bot **55**: 49–57

Nunes-Nesi A, Carrari F, Gibon Y, Sulpice R, Lytovchenko A, Fisahn J, Graham J, Ratcliffe RG, Sweetlove LJ, Fernie AR (2007) Deficiency of mitochondrial fumarase activity in tomato plants impairs photosynthesis via an effect on stomatal function. Plant J **50**: 1093–106

Nunes-Nesi A, Carrari F, Lytovchenko A, Smith AMO, Loureiro ME, Ratcliffe RG, Sweetlove LJ, Fernie AR (2005) Enhanced photosynthetic performance and growth as a consequence of decreasing mitochondrial malate dehydrogenase activity in transgenic tomato plants. Plant Physiol **137**: 611–22

Okumoto S, Schmidt R, Tegeder M, Fischer WN, Rentsch D, Frommer WB, Koch W (2002) High affinity amino acid transporters specifically expressed in xylem parenchyma and developing seeds of Arabidopsis. J Biol Chem **277**: 45338–45346

Palmieri F (1994) Mitochondrial carrier proteins. FEBS Lett **346**: 48–54

Palmieri F (2004) The mitochondrial transporter family (SLC25): Physiological and pathological implications. Pflugers Arch Eur J Physiol **447**: 689–709

Palmieri F, Indiveri C, Bisaccia F, Iacobazzi V (1995) Mitochondrial metabolite carrier proteins: Purification, reconstitution, and transport studies. Methods Enzymol **260**: 349–369

Palmieri F, Pierri CL (2010) Structure and function of mitochondrial carriers - Role of the transmembrane helix P and G residues in the gating and transport mechanism. FEBS Lett **584**: 1931–1939

Palmieri F, Pierri CL, De Grassi A, Nunes-Nesi A, Fernie AR (2011) Evolution, structure and function of mitochondrial carriers: A review with new insights. Plant J **66**: 161–181

Palmieri F, Rieder B, Ventrella A, Blanco E, Do PT, Nunes-Nesi A, Trauth a U, Fiermonte G, Tjaden J, Agrimi G, et al (2009) Molecular identification and functional characterization of Arabidopsis thaliana

mitochondrial and chloroplastic NAD+ carrier proteins. J Biol Chem **284**: 31249–31259

Palmieri L, Lasorsa FM, De Palma A, Palmieri F, Runswick MJ, Walker JE (1997) Identification of the yeast ACR1 gene product as a succinate-fumarate transporter essential for growth on ethanol or acetate. FEBS Lett **417**: 114–118

Palmieri L, Picault N, Arrigoni R, Besin E, Palmieri F, Hodges M (2008a) Molecular identification of three Arabidopsis thaliana mitochondrial dicarboxylate carrier isoforms: organ distribution, bacterial expression, reconstitution into liposomes and functional characterization. Biochem J **410**: 621–629

Palmieri L, Santoro A, Carrari F, Blanco E, Nunes-Nesi A, Arrigoni R, Genchi F, Fernie AR, Palmieri F (2008b) Identification and Characterization of ADNT1, a Novel Mitochondrial Adenine Nucleotide Transporter from Arabidopsis,. Plant Physiol **148**: 1797–1808

Picault N, Hodges M, Palmieri L, Palmieri F (2004) The growing family of mitochondrial carriers in Arabidopsis. Trends Plant Sci **9**: 138–146

Picault N, Palmieri L, Pisano I, Hodges M, Palmieri F (2002) Identification of a novel transporter for dicarboxylates and tricarboxylates in plant mitochondria: Bacterial expression, reconstitution, functional characterization, and tissue distribution. J Biol Chem **277**: 24204–24211

Pilkington SM, Encke B, Krohn N, Hönhne M, Stitt M, Pyl ET (2015) Relationship between starch degradation and carbon demand for maintenance and growth in Arabidopsis thaliana in different irradiance and temperature regimes. Plant Cell Environ **38**: 157–171

Popova TN, Pinheiro de Carvalho MÂA (1998) Citrate and isocitrate in plant metabolism. Biochim Biophys Acta - Bioenerg **1364**: 307–325

Pracharoenwattana I, Cornah JE, Smith SM (2005) Arabidopsis peroxisomal citrate synthase is required for fatty acid respiration and seed germination. Plant Cell **17**: 2037–48

Pracharoenwattana I, Cornah JE, Smith SM (2007) Arabidopsis peroxisomal malate dehydrogenase functions in β-oxidation but not in the glyoxylate cycle. Plant J **50**: 381–390

Raymond P, Spiteri A, Dieuaide M, Gerhardt B, Pradet A (1992)

Peroxisomal beta-oxidation of fatty acids and citrate formation by a particulate fraction from early germinating sunflower seeds. Plant Physiol Biochem **30**: 153–161

Salon C, Raymond P, Pradet A (1988) Quantification of carbon fluxes through the tricarboxylic acid cycle in early germinating lettuce embryos. J Biol Chem **263**: 12278–12287

Scalise M, Pochini L, Giangregorio N, Tonazzi A, Indiveri C (2013) Proteoliposomes as tool for assaying membrane transporter functions and interactions with xenobiotics. Pharmaceutics **5**: 472–97

Sienkiewicz-Porzucek A, Nunes-Nesi A, Sulpice R, Lisec J, Centeno DC, Carillo P, Leisse A, Urbanczyk-Wochniak E, Fernie AR (2008) Mild reductions in mitochondrial citrate synthase activity result in a compromised nitrate assimilation and reduced leaf pigmentation but have no effect on photosynthetic performance or growth. Plant Physiol **147**: 115–27

Sienkiewicz-Porzucek A, Sulpice R, Osorio S, Krahnert I, Leisse A, Urbanczyk-Wochniak E, Hodges M, Fernie AR, Nunes-Nesi A (2010) Mild reductions in mitochondrial NAD-dependent isocitrate dehydrogenase activity result in altered nitrate assimilation and pigmentation but do not impact growth. Mol Plant **3**: 156–73

Sulpice R, Sienkiewicz-Porzucek A, Osorio S, Krahnert I, Stitt M, Fernie AR, Nunes-Nesi A (2010) Mild reductions in cytosolic NADP-dependent isocitrate dehydrogenase activity result in lower amino acid contents and pigmentation without impacting growth. Amino Acids **39**: 1055–1066

Sze H, Geisler M, Murphy AS (2014) Linking the evolution of plant transporters to their functions. Front Plant Sci **4**: 547

Yoo C-M, Quan L, Blancaflor EB (2012) Divergence and Redundancy in CSLD2 and CSLD3 Function During Arabidopsis Thaliana Root Hair and Female Gametophyte Development. Front Plant Sci **3**: 1–17

Zelitch I (1988) Synthesis of Glycolate from Pyruvate via Isocitrate Lyase by Tobacco Leaves in Light. Plant Physiol **86**: 463–8

SUPPLEMENTAL DATA

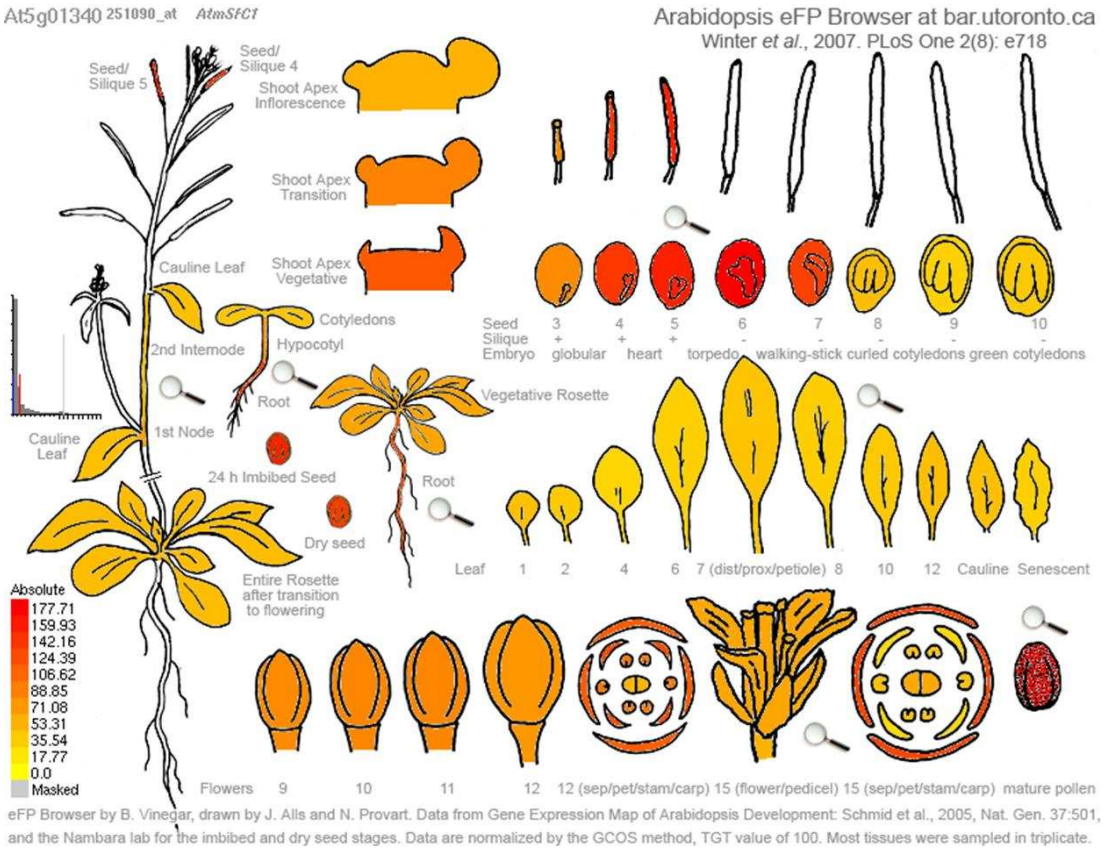

Supplemental Figure 1. In silico analyses of the *AtSFC1* gene in different tissues. Arabidopsis eFP Browser (http://bar.utoronto.ca/ef/cgi-bin/efpWeb.cgi).

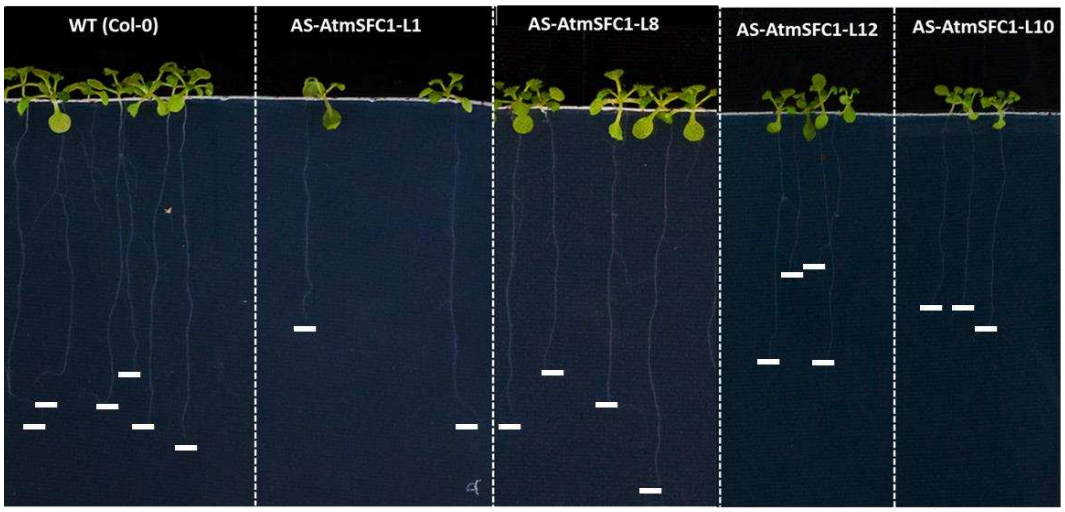

Supplemental Figure 2. Root length of antisense lines AtSFC1 grown on vertical agar plates. Solid white bars represents the limit of the root.

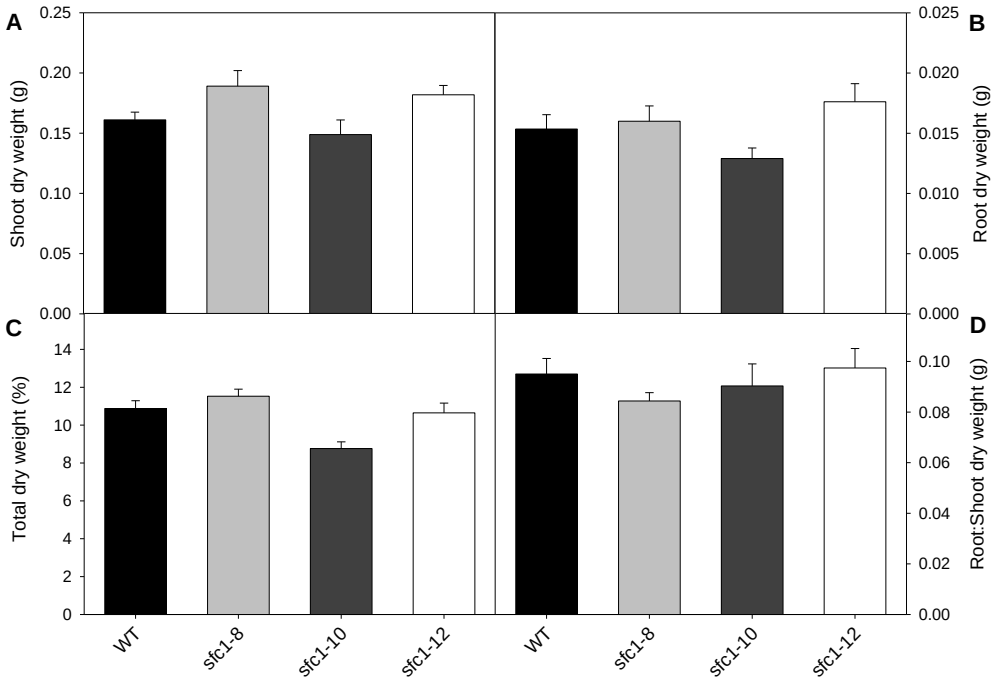

Supplemental Figure 3. Growth parameters of antisense lines of *At*SFC1. **(A)** Shoot dry weight, **(B)** Root dry weight, **(C)** Total dry weight, **(D)** Root:Shoot dry weight. Values are means ± SE of six individual determinations per line. An asterisk indicates values that were determined by the Studen's *t*-test to be significantly different ($P < 0.05$) from the wild-type.

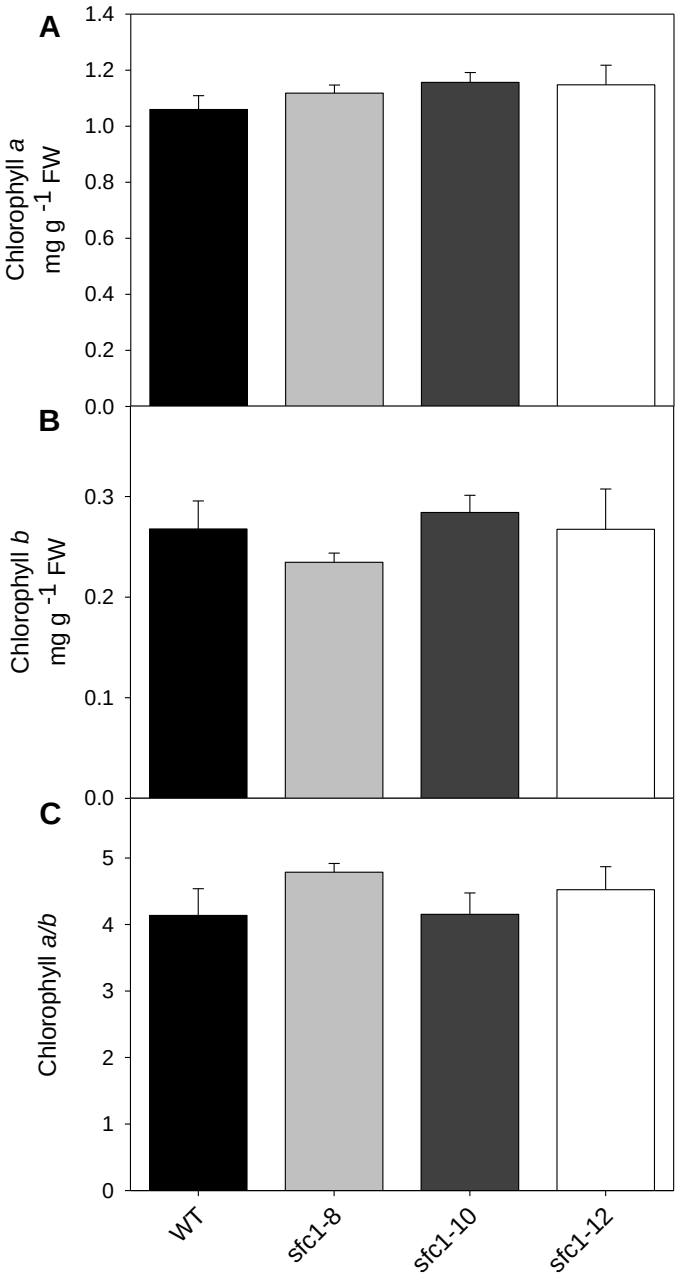

Supplementary Figure 4. Alterations in the levels of photosynthetic pigments in plant leaves of antisense lines *AtSFC1.* **(A)** levels of chlorophyll *a*, **(B)** levels of chlorophyll *b*¸ **(C)** chlorophyll a:b ratio. Values are means ± SE of six individual determinations per line.

CHAPTER 2

Deficiency in alternative respiration pathway induces changes on OXPHOS system under carbohydrate starvation in Arabidopsis cell suspensions culture

ABSTRACT

BRITO, Danielle Santos, D.Sc., Universidade Federal de Viçosa, August, 2016. **Deficiency in alternative respiration pathway induces changes on OXPHOS system under carbohydrate starvation in Arabidopsis cell suspensions culture.** Advisor: Adriano Nunes Nesi.

Alternative substrates such as amino acids can directly feed electrons into the mitochondrial electron transport chain (mETC) via the electron transfer flavoprotein/electron-transfer flavoprotein: ubiquinone oxidoreductase (ETF/ETFQO) complex, which supports respiration during stress situations including carbohydrate limitation and drought. Here, by using a cell culture we investigated the responses of *Arabidopsis thaliana* mutants deficient in the expression of ETFQO following carbon limitation supplied with amino acids. Our results revealed that in absence of the ETFQO protein increased activity of complex I and II and that similar reduction in the activity of complex III and IV compared to wild type following carbohydrate limitation is observed. Supplementation with branched chain amino acids (BCAA) did not lead to increases in the activities of complexes III and IV in mutant cells. Our results also demonstrated that isovaleryl-CoA dehydrogenase (IVDH) activity is induced during carbohydrate limitation only in wild type and that these changes occurred concomitantly with enhanced amount of proteins. By contrast, the activity and total amount of IVDH was not altered in mutant cells. Taken together, our findings indicate that the lack of ETFQO protein disrupt electron donation from BCAA to the mETC following carbohydrate starvation and consequently compromise oxidative phosphorylation system and alternative respiration as demonstrated here by impairments in IVDH function.

Keywords: Alternative pathway; carbon starvation; electron transfer flavoprotein: ubiquinone oxidoreductase; mitochondria.

INTRODUCTION

Aerobic respiration is the most important process used to produce energy for cells (Millar et al., 2005; Plaxton and Podestá, 2006). Respiratory process in plants involves a combination of different metabolic pathways that includes glycolysis, tricarboxylic acid (TCA) cycle and oxidative phosphorylation (OXPHOS) (Millar et al., 2011). These processes are of significance in a variety of physiological functions as ATP generation, provision of carbon skeletons for biosynthetic processes, photorespiration (Millar et al., 2011). However, the respiratory metabolism itself is much more complex than previously thought. Thus, several others alternatives pathways can supply substrates for the TCA cycle reactions as well as a range of dehydrogenases that can directly or indirectly donate electrons for the mitochondrial electron transport chain (mETC) (Araújo et al., 2011b; Schertl and Braun, 2014; Hildebrandt et al., 2015). This is reasonable to assume that, collectively, it makes the respiratory metabolism extremely flexible under several stress conditions (Araújo et al., 2011a; van Dongen et al., 2011). It should be noted that, among the possible substrates for mitochondrial respiration in plants, which includes proteins, lipids and chlorophylls (Ishizaki et al., 2005; Ishizaki et al., 2006; Araújo et al., 2010), compelling evidence, has demonstrated that proteins and amino acids are preferably used for energy generation during stressful situations (Araújo et al., 2010; Araújo et al., 2011a; Araújo et al., 2011b; Kirma et al., 2012).

In this context, it has been shown that BCAA (isoleucine, leucine and valine) can be used as alternative substrates (Araújo et al., 2010; Gu et al., 2010; Kochevenko et al., 2012), and subsequently, supply of electrons to the mETC by action an alternative pathway, ETF/ETFQO (Electron transfer flavoprotein: flavoprotein ubiquinone oxidorreductase) system (Heazlewood et al., 2004b; Watmough and Frerman, 2010). ETF is a heterodimeric protein composed of two subunits, α and β and is localized in the mitochondrial matrix. ETFQO is associated with the inner mitochondrial membrane and have a three functional domains that bind the FAD, ubiquinone (UQ) redox centers and iron-sulfur $[4Fe\text{-}4S]^{2+1+}$ cluster domain near its C terminus that is likely to be

required for electron flow from flavin to UQ. Electrons derived from the various dehydrogenation reactions are transferred from ETF to ETFQO at the iron–sulfur cluster and subsequently to the FAD co-factor. (Ishizaki et al., 2005; Watmough and Frerman, 2010). FAD is the electron donor to UQ in the inner mitochondrial membrane (Ishizaki et al., 2005; Watmough and Frerman, 2010).

Nevertheless, how exactly the electron donation and whether other component for this alternative system are present in plants, still remains to be elucidated. In mammals at least 11 mitochondrial dehydrogenases, able to donate electrons to the electron transport chain via ETFQO, have been identified to date (Watmough and Frerman, 2010). In plants, only two enzymes, 2-hydroxyglutarate dehydrogenase (D-2HGDH) and isovaleryl-CoA dehydrogenase (IVDH) associated with the ETF / ETFQO system (Engqvist et al., 2009; Araújo et al., 2010) have been identified thus far. D-2HGDH, located in the mitochondrial matrix, catalyze the oxidation of 2-hydroxyglutarate to 2-oxoglutarate reducing $FADH_2$, which can be regenerated via ETF (Engqvist et al., 2009). In addition to D-2HGDH, IVDH, another mitochondrial matrix enzyme, are linked to the degradation of the BCAA (Ding et al., 2012). Analyses of Arabidopsis mutants lacking D-2HGDH and IVDH enzymes following carbon starvation conditions suggest that these dehydrogenases are involved in the generation of energy from protein degradation using amino acids generated (preferably valine, leucine, isoleucine and lysine) as electrons sources (Araújo et al., 2010).

Compelling evidence has demonstrated that following carbohydrate starvation during dark-induce senescence the ETFQO transcripts are increased (Ishizaki et al., 2005). In addition, by using T-DNA knockout mutants it was demonstrated that accelerated senescence as compared to wild type is usually observed in those knockout plants (Ishizaki et al., 2005; Ishizaki et al., 2006; Araújo et al., 2010; Pires et al., 2016). Interestingly, the ETF transcripts levels remained unchanged during carbon starvation (Ishizaki et al., 2006). This fact apart, phenotypic and metabolic characterization of both ETF and ETFQO mutants is quite similar (Ishizaki et al., 2006) suggesting a functional association between them to support plant respiration during energetic stress.

Although the function of the ETF/ETFQO system is not yet fully understood, it clearly plays a key role during the oxidation of alternative respiratory substrates, particularly when the plants are under stress conditions, such as carbon limitations and osmotic (Lehmann et al., 2009; Pires et al., 2016) as well as in situations typically experienced by plants during their normal growth (Araújo et al., 2010). Altogether, these evidences has pointed out to the suggestion that the ETF/ETFQO system seems to be essential for plants outlive during stress situations such as a carbon depletion.

We suppose that the inactivation of the ETFQO protein will impair the transference of electrons generated by the oxidation of BCAA to the ubiquinol pool via this system affecting the mETC activity as well as the activity of other electrons donors components such as IVDH. For this reason and in an attempt to elucidate how exactly the OXPHOS system is reorganized following sucrose depletion a molecular, metabolic and physiological approach was undertaken to study ETFQO mutants. Here we investigated the role of ETFQO under carbohydrate starvation conditions as well as the role of BCAA as alternative substrates to fulfill respiration into mitochondrial metabolism during carbohydrate deprivation. We carried out a range of experiments using Arabidopsis cell culture following carbon starvation and supplied with BCAA as alternative substrates. Our findings revealed that the activities of the protein complexes of the respiratory chain for both mutant and wild type are differently affected in response to carbohydrate starvation. Our results also show that the IVDH activity is not induced following sucrose limitation conditions in the absence of the ETFQO and that changes in the activity of IVDH are concomitantly with changes in the protein amount.

MATERIAL AND METHODS

Cultivation of *Arabidopsis* cell suspension cultures

All experiments were carried out using *Arabidopsis thaliana* from the Columbia ecotype (Col-0). Establishment of an *A. thaliana* cell culture was carried out as described by May and Leaver, (1993). Briefly, *A. thaliana* seeds were surface sterilized and imbibed for 2 days at 4 ℃ in the dark on 0.8% (*w*/*v*) agar plates containing half-strength medium (pH 5.7) (Murashige and Skoog, 1962). Seeds were subsequently germinated under long-day conditions (16 h light/8 h dark) at 100 µmol photons m^{-2} s^{-1}. After ten days, seedlings were cutted into small pieces (3 cm^2) by placing on plates with callus induction medium (Gamborg B5, pH 5.7, sucrose 3% [*w/v*], agar 0.8% [*w/v*], 2,4-dichloropenoxyacetic acid 0.0001% [*w/v*] and kinetin 0.00001% [*w/v*]) and growing in the dark for three weeks. Suspension cultures were established by transference of white callus to 500-mL flasks containing 100 mL of B5 liquid medium as described above. Cells were cultivated at 24-26 ℃ under rotary shaker (90 rpm) in the dark. To maintain the cells in optimal conditions, the medium was renovated every seven days. The T-DNA mutant line SALK_007870 (*etfqo-1*, background ecotype Col-0, Ishizaki et al., 2005) used in this study were handled exactly as previously described.

Treatment of *Arabidopsis* cell suspension cultures

The cell suspension cultures were treated in two different conditions of carbohydrate limitation. Both were performed without adding carbon source (sucrose), but one of them was added 30 mM of branched chain amino acids – BCAA (10 mM of each one, valine, leucine and isoleucine), as alternative carbon source for respiration. Control cell cultures were treated with 3% of sucrose. After 24 hours under these conditions, the cells were collected for isolation of mitochondria, rate growth procedures, measurements of respiration, determination of enzyme activities and as well as immunoblotting analysis. The starting material for mitochondrial isolations was ca 40 g cells.

Genotype characterization and analysis of ETFQO mRNA expression by RT-PCR

The mutant line, SALK_007870 (*etfqo-1*), obtained gently donated by Dr. Alisdair R. Fernie (Max-Planck Institute of Molecular Plant Physiology, Potsdam-Golm, Germany) was checked by PCR analysis using specific primers for the *ETFQO* open reading frame (forward primer *etfqo-1,* L1 5'-AAGGTGGTACCGTGCTTCAG-3' and reverse primer *etfqo-1,* R1 5'-CACCACCTTCAGGCACTGTC-3') and primers specific for the insertion elements (LBa1 5'-TGGTTCACGTAGTGGGCCATCG-3') (Ishizaki et al., 2005). The PCR reactions were performed with Taq DNA polymerase (Invitrogen) according to manufacturer's instructions, in a thermocycler programmed to perform an initial denaturation at 94 ℃ for 2 minutes, 35 cycles at 94 ℃ for 30 seconds; 58 ℃ for 1 minute and 72 ℃ for 45 seco nds and a final extension of 72 ℃ for 5 minutes. The PCR products were analyzed in electrophoresis on 2% (w/v) agarose gel to confirm the mutant genotype. For semiquantitative expression analysis, total RNA was isolated from cell suspension cultures cultivated under carbohydrate limitation during 24 hours using TRizol Reagent (Invitrogen) according to manufacturer's recommendations. First-stand cDNA was synthesized from 4 µg of total RNA using the oligo dTv primer and MMLV reverse transcriptase (Promega). PCR amplification of the cDNA encoding the ETFQO of Arabidopsis (At2g43400) was performed using primers specific for the open reading frame, L1 and R1, described above. PCR amplification of the cDNA encoding the Actin of Arabidopsis (ACT2, At3g18780) was performed with forward primer 5'-TGGAAAAGATCTGGCATCACAC-3' and reverse primer 5'-GAACCACCGATCCAGACACT-3', as a housekeeping gene control.

Quantitative Real-Time PCR

Quantitative Real Time PCR analysis was performed according to (Welchen et al., 2012). Total RNA was isolated from cell suspensions, which were harvested at intervals of 3, 6, 12, 24, 72 and 168 hours after application of treatments. For the experiments, defined amounts of sucrose or amino acids

were added. Specifically, cell cultivation took place at the following four conditions: (i) control (3% sucrose), (ii) sucrose-free, (iii) sucrose-free plus BCAA (without sucrose plus 10 mM of each BCAA; and (iv) plus sucrose plus BCAA (plus 3% sucrose plus 10 mM of each BCAA) for 24 hours.

The extraction of RNA was performed using TRizol Reagent (Invitrogen) according to manufacturer's recommendations. To confirm the absence of genomic DNA contamination, a quantitative PCR analysis was carried out using samples no-treated with reverse transcriptase enzyme. The integrity of the RNA was checked on 2% w/v agarose gels, and the concentration was measured before and after DNase I digestion using Gen5 Data Analysis Software (BioTek®). cDNA was synthesized from 4 µg total RNA using the oligo dTv primer and MMLV reverse transcriptase (Promega). PCR reactions were performed using an ABI PRISM 7900 HT sequence detection system (Applied Biosystemshttp://www.appliedbiosystems.com/) and Platinum® SYBR® Green qPCR SuperMix-UDG with ROX. Fluorescence was measured at 72 ℃ during 40 cycles. Relative transcript levels were calculated by a relative quantification (standard curve method). The amplification was performed using specific primers for IVDH cDNA forward primer (5'-CTGTTGCGAGGGACTGTGACAATG-3') and reverse primer (5'-GAATAGTTCCGGCGCAGTCCTTTG-3'); for ETFQO cDNA forward primer (5'-TGCAGATCAACGCTCAAAAC-3') and reverse primer (5'-ACCTTCAGGCACTGTCCACT-3'); for ETFβ cDNA forward primer (5'-CAGGACAGATGGTTGCAGCTTTAC-3') and reverse primer (5'-CCAACACAACCTTCGATGCAAACG-3') and for D2HGDH cDNA forward primer (5'-TTTCTGATGGTGTAATCGCTC-3') and reverse primer (5'-TGCTTTCTGTAACGCCTCTG-3') normalize gene expression, the constitutively expressed F-box was amplified using the following primers: forward 5'-GTCCTTTAGGTCGAGTTGGGTCG-3'; and reverse 5'-GGCCCATGAGATGACACATTTGAGT-3'.

Growth experiments

Starting point of growth experiments was the transfer of 1.5 g of *Arabidopsis thaliana* col-0 cells into fresh suspension cell medium. The three

cultivation conditions were as described above. Weight increase was determined after 24 h.

Respiration measurements

Dark respiration of the cell cultures was measured in an oxygen electrode following a protocol detailed previously (Geigenberger et al., 2000). Measurements took place in a 1 ml reaction vessel for about 5 minutes and were based on 30 mg cells. Oxygen depletion in the buffer was kept to less than 20% of the initial value. Potassium cyanide (1 mM KCN) was used for cytochrome c oxidase inhibition and salicylhydroxamic acid (750 µM SHAM) for inhibition of Alternative oxidase (AOX).

Isolation of mitochondria

Preparations of mitochondria were performed according to Schertl et al., (2014). Six parallel preparations were carried out for Arabidopsis cell suspensions cultivated at the three different conditions outlined above. Starting material was ca. 40 g cells per condition. In brief: Arabidopsis cells were disrupted in a Waring blender in buffer containing 450 mM sucrose, 15 mM 3-(*N*-morpholino)propanesulfonic acid (MOPS), 1.5 mM EGTA, 0.6 (*w*/*v*) polyvinylpyrrolidone (PVP-40), 0.2% bovine serum albumin (BSA), 0.2% phenylmethylsulfonyl fluoride (PMSF), pH 7.4 (KOH). To remove cell debris the suspensions were centrifuged twice for 5 min at 2.700 g and once for 10 min at 8300 g. Afterwards, the supernatants containing the mitochondrial fractions were transferred to a new tube for a high speed centrifugation at 17.000 g for 10 min. The mitochondrial pellets were resuspended in 3 mL of washing buffer containing 300 mM sucrose, 10 mM MOPS, 1 mM EGTA, 0.2 mM PMSF, pH 7.2 (KOH). Next, the mitochondrial suspensions were carefully placed on Percoll gradients and centrifuged for 90 min at 70.000 *g* using an ultracentrifuge. After centrifugation the bands representing the mitochondria were transferred into new tubes using a Pasteur pipette. The mitochondrial fractions were washed three times in resuspension buffer containing 400 mM mannitol, 10 mM Tricine, 1 mM EGTA, 0.2 mM PMSF, pH 7.2 (KOH) at by

centrifugation at 14300 *g* for 10 min. All steps were carried out at 4 ℃. Isolated mitochondria were aliquoted and stored at -80 ℃.

Measurements of enzyme activities

All enzyme assays were carried out in final volumes of 300 µL at 25 ℃ using an Epoch Microplate Spectrophotometer (Biotech, Winooski, VT, USA). Mitochondrial suspensions stored at -80 ℃ were used to quantify the mitochondrial enzyme activities. First, mitochondrial suspensions were thawed and then centrifuged for 10 min at 25000 g. The supernatants (soluble fractions) were recovered in a new microtube. The pellets were suspended in resuspension buffer (membrane fraction) and protein quantifications were carried out for both the soluble and the membrane fractions using the Bradford method (Bradford, 1976).

IVDH activity was monitored by following the reduction of dichlorophenolindophenol (DCIP) (E = 19.1 mM^{-1} cm^{-1}) at 600 nm. The reaction mixture contained 250 mM Tris-HCl pH 7.5, 1 mM KCN, 166 µM FAD, 0.06 mM DCIP, 1 mM PMS and 20 µg of soluble mitochondrial proteins. The reaction was started by adding 67 µM Acyl-CoA.

To determine OXPHOS system activities we used the membrane fractions. Complex I and alternative NADH dehydrogenase activities were measured according to Birch -Machin et al. (1994). Mitochondrial proteins (5 µg) were suspended in a buffer containing 0.25 mM Tris-HCl pH 7.5, 2 mM KCN, 2 µg/mL Antimycin A, 0.2 mM NADH, 200 µM ubiquinone (oxidized). Complex I activity was measured by following the decrease in absorbance due to the oxidation of NADH at 340 nm (E=6.2 $mM^{-1}.cm^{-1}$). The specific activity of complex I was measured before the addition of 2 µg/ml rotenone. Complex II was measured according to Birch-Machin et al. (1994). For this assay, 15 µg of membrane protein was suspended in a buffer including 50 mM Tris-HCl pH 7.4, 5 mM $MgCl_2$, 20 mM succinate, 0.3 mM ATP, 0.5 mM SHAM, 100 µM decylubiquinone (oxidased) and 2 mM KCN. The reaction was started with 50 µM DCIP and the activity of Complex II was monitored by the reduction of DCIP (E =19.1 mM^{-1} cm^{-1}) at 600 nm. Complex III activity was measured according Birch-Machin et al. (1994) and the preparation of Decylubiquinol according to

Lang and Packer, (1987). The assay was carried out with 2 µg of protein from mitochondrial membrane fraction and took place in a buffer including 50 mM Tris-HCL pH 7.4, 5 mM $MgCl_2$, 2.5 mg/mL BSA, 2 mM KCN, 15 µM oxidized cytochrome c, 0.005 µg/µL Rotenone, 35 µM decylubiquinone. Enzyme activity was followed at 550 nm for 10 minutes. Complex IV activity was measured according to Birch-Machin et al. (1994). The assay mixture contained 50 mM Tris-HClpH 7.4, 15 µM cytochrome c (reduced with sodium dithionite). Protein (1µg of membrane proteins) was used to start the reaction and oxidation of cytochrome c (E = 19 mM^{-1} cm^{-1}) was monitored at 550 nm.

Gel electrophoresis and immunoblotting analysis

One-dimensional Glycine SDS-PAGE was carried out as outlined by Laemmli, (1970) using an XCell SureLock Mini-Electrophoresis System (Life Technologies GmbH). Mitochondrial proteins were quantified using a microplate assay using the Coomassie Protein Assay kit (Biorad, City, Country). The proteins were loaded Novex® 10–20% Tris-Glycine Mini Gels (Invitrogen™) according to manufacturer's recommendations. Afterwards, the proteins were, immediately, transferred onto nitrocellulose membrane using a Semi-Dry Transfer system (Bio-Rad, USA). The transfer of proteins was carried out according Schertl et al. (2014) at 25 V, 152 mA for about 90 min using transfer buffer (25mM Tris, 192 mM glycine, 1.3 mM SDS, 20% Methanol). The blots were rinsed several timers in TTBS buffer (0.1 M Tris-HCl pH 7.5, 0.155 M NaCl and 0.01% (*v*/*v*) Tween 20) to remove all methanol and then incubated with 1: 1000 primary antibody dilution in TTBS buffer for about 16 h at room temperature. Antibody IVDH was used following technical instruction of Proteintech, USA. Subsequently, membranes were incubated for 2 h with a 1: 800 diluted secondary antibody directly coupled to the horseradish peroxidase. All blotts were detected using the ECL prime chemiluminescence detection kit from GE Healthcare (Munich, Germany).

Statistical analysis

The experiments were conducted in a completely randomized design with three replicates of each genotype. Data were evaluated by variance analysis and tested for significance differences ($P < 0.05$) using Student's *t* tests and Tukey's test (P<0.05). All statistical analyses were performed using algorithms embedded into Microsoft Excel®.

RESULTS

Confirmation of the mutant *etfqo* of *Arabidopsis* cell suspension cultures

To investigate *in vivo* the function of ETFQO protein, cell cultures were generated from a mutant line previously shown to lack the ETFQO protein. The line chosen for this study, *etfqo-1*, has a T-DNA insertion in the 13nd exon region (Figure 1A) and have been previously characterized in detail (Ishizaki et al., 2005). The insertional element in the *etfqo-1* is positioned upstream of the iron-sulfur cluster and it is expected that the electron transfer capacity would be severely compromised in this line. Homozygous lines were confirmed by genomic PCR using specific primers for open reading frame of the gene *ETFQO* in combination with the primer for the T-DNA left border. After the genetic confirmation, homozygous cell cultures were subjected to carbon deprivation for 24 hours and then expression analysis by RT-PCR were performed. The actin gene was used as a control to demonstrate integrity of the RNA preparation and that similar amount of RNA was used. Transcripts for *ETFQO* gene were detected only in wild type (ecotype Col-0) plants, whereas no amplification product was observed in the mutant line (Figure 1B). These results confirmed that the cells used in this study are knock out mutants.

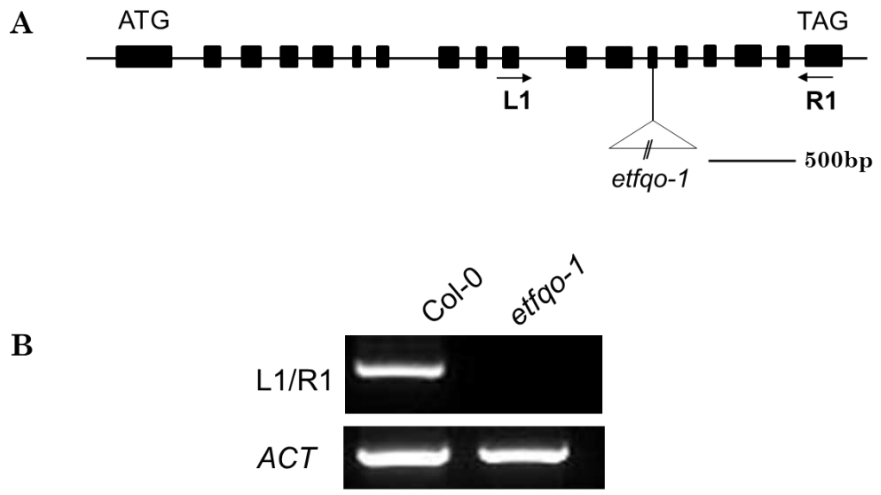

Figure 1. Identification of *etfqo*-1 mutant**. (A)** Genomic structure of ETFQO loci. Arrows represent positions of primers used for genotype and RT-PCR analyses of wild-type and mutant line. Black boxes indicate exons. In *etfqo-1* mutant, the T-DNA is inserted in exon 13. **(B)** RT-PCR analysis on total RNA from wild-type (Col-0) and the mutant line *etfqo-1* from cell culture. Was used 4ug of total RNA.

Wild type and *etfqo* mutants exhibited the same pattern of cell growth under carbohydrate starvation

All organisms are dependent on nutrients from the environment for their continuous viability and growth and maintenance these mechanisms are energy dependent. Suspension cell culture was chosen for initial studies on sucrose starvation because the cells lack mature plastids and are incapable of photosynthesis. The cells are therefore dependent on the presence of sucrose in the growth medium as their sole source of carbon. Briefly, cell cultivation was performed following three conditions: (i) control (3% sucrose), (ii) sucrose-free, (iii) sucrose-free plus BCAA (without sucrose plus 10 mM of each BCAA; and (iv) plus sucrose plus BCAA (plus 3% sucrose plus 10 mM of each BCAA). After cultivation for 24 hours in the conditions described above we analyzed cell growth. The cell growth of both genotypes was quite similar (Figure 2) and no significant differences between them under the conditions analyzed in this study were observed. However, following carbohydrate limitation was not

observed an increase in the fresh cell weight for both the wild type and to the *etfqo*-1 (Figure 2A and 2B, respectively) when compared with the others treatments was observed.

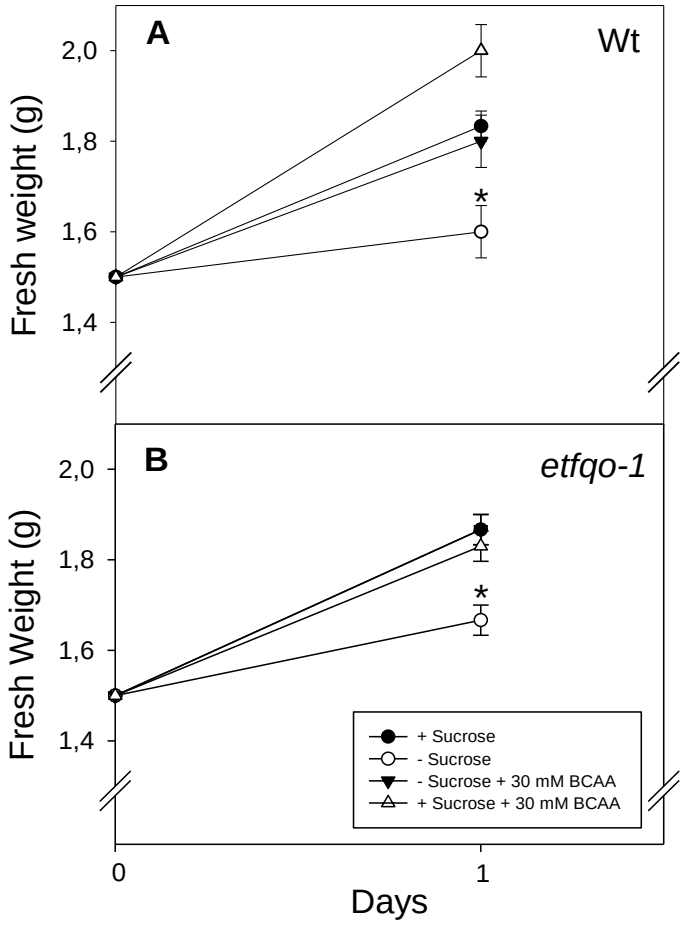

Figure 2. Cell growth under sucrose-starvation conditions in Arabidopsis cell suspension culture**. (A)** Growth in Wt, **(B)** Growth in *etfqo*-1 mutants. The growth measurements were based on the fresh cell weight values of *A. thaliana* expressed in grams carried out after cultivation for 0h and 24h at the following conditions: 1) plus sucrose, 3% [w/v]; 2) no sucrose; 3) no sucrose plus 30mM of BCAA (10 mM of each, Valine, Isoleucine and Leucine) and 4) plus sucrose plus 30 mM of BCAA. Standard errors are based on three biological replicates. Asterisk indicates values that were determined by the Student's *t* test to be significantly different ($P < 0.05$) between the treatments for each genotype.

Respiration is affected in *etfqo* mutants following carbohydrate starvation

To investigate the impact of carbohydrate limitation in mitochondrial respiration coupled with the role of amino acid degradation as alternative sources of electrons to the mETC, oxygen consumption measurements were performed in cells submitted to 24-hour carbon starvation. Our results revealed that wild type cells under sucrose limitation displayed reduction on respiratory rates of approximately 53% (Table 1). The respiratory rates of *etfqo*-1 is significantly lower under all conditions analyzed here in comparison with that observed for wild type cell, excepted for the treatment plus sucrose and plus BCAA it was similar than wild type for the same treatment.

To enhance our understanding of the above-described results, we next analyzed the effects of two different electron transport chain inhibitors by using 1mM KCN (potassium cyanide), inhibitor of cytochrome *c* oxidase (complex IV), and 750 µM SHAM (salicylhidroxamic acid), an inhibitor of the alternative oxidase (AOX). Our results revealed that the application of KCN inhibited significantly the respiration of the cells grown in all conditions analyzed for both wild-type and *etfqo*-1 (Table 1). It was also observed that in cells treated with sucrose and BCAA were less affected by this inhibitor presenting a reduction of 26% and 16% for wild type and *etfqo*-1, respectively. In concerning the application of KCN plus SHAM, the oxygen consumption was not significantly affected only in *etfqo*-1 cells growing without sucrose for up to 24 h.

Table 1: Oxygen consumption measurements in cells from *Arabidopsis thaliana*

	O_2 Consumption (nmol O_2 $^{-1}$ g^{-1} of cell culture min^{-1})							
	Wild Type				*etfqo-1*			
	+ Suc	- Suc	- Suc + BCAA	+ Suc + BCAA	+ Suc	- Suc	- Suc + BCAA	+ Suc + BCAA
No Inhibitor	715.8 ± 17.8a	437.3 ± 13.7b	378.8 ± 13.6b	619.9 ± 38.6a	**582.4 ± 14.5**ab	**516.0 ± 19.2**bc	**480.8 ± 7.2**c	620.8 ± 23.3a
KCN	309.2 ± 22.0b*	250.8 ± 21.8b*	270.2 ± 11.3b*	456.5 ± 18.1a*	225.4 ± 14.9c*	271.0 ± 14.5c*	341.8 ± 6.8b*	520.6 ± 19.0a*
SHAM	181.2 ± 10.4b*	160.2 ± 5.9b*	173.8 ± 6.6b*	240.3 ± 13.3a*	153.7 ± 15.7b*	232.4 ± 12.2a	243.8 ± 8.6a*	237.1 ± 10.0a*

Oxygen consumption measurements in cells suspension from *Arabidopsis thaliana* cultivated in four different treatments for 24 hours. Values presented are mean ± SE of three different samples obtained at the same cultivation. Values in boldface were determined by Student's *t* test to be significantly different ($P < 0.05$) from the wild type in the condition no inhibitor. The same letters indicates no difference significant ($P < 0.05$, Tukey's test) between treatments for each genotype in the same condition. The asterisk indicates difference significant ($P < 0.05$) determined by Student's *t* test for the effect of inhibitor in the same treatment for each genotype. Inhibitors of cytochrome c oxidase (potassium cyanide [KCN]) and the alternative oxidase (salicylhydroxamic acid [SHAM]) were added at defined time points (see Material and Methods).

Activities of the Complex I and Complex II it was much higher in *etfqo* than in the wild type under carbohydrate starvation

In order to evaluate the role of the alternative electron transport during stress situations, and to better understand this transient reconfiguration in the respiratory metabolism during carbohydrate limitation, a range of assays were carried out to analyze the activity of complexes I, II, III and IV of the mETC (Figure 3). Accordingly, to each assay performed following the isolation of mitochondria from cell culture previously subjected to the three different treatments, soluble and membrane fractions were used. The complex I activity was significantly affected under sucrose limitation mainly for wild type cell. The *etfqo*-1 suffered only a slight reduction in the complex I activity on cells treated without sucrose and with sucrose and plus BCAA. It should be noted, however, that in all conditions analyzed here, complex I activity was higher in mutant cells than in wild type ones (Figure 3A). The alternative NADH dehydrogenase was reduced in all conditions analyzed in the *etfqo*-1 when compared with wild type (Figure 4). Given that both complex I and alternative NADH dehydrogenases use the same substrate, NADH, the activity of complex I was inhibited by the addition of rotenone, allowing us to distinguishing between the activity of complex I and the ones of the alternative NADH dehydrogenase (Figure 4). Differently from the observed for the complex I activity, the activity of the complex II does not seems to be affected under carbohydrate limitation in wild type cells. However, when compared to the control (wild type in the presence of sucrose, Figure 3B) the activity of complex II is about five times greater in *etfqo*-1 cells. Interestingly, treatment without sucrose and supplemented with BCAA showed the lower activity of complex II in mutant plants, although this activity was still higher than in the wild type ones.

By analyzing the activity of the complex III we noticed that it was not significantly altered in wild type cells under all conditions (Figure 3C), whereas the opposite was observed in mutant cells. Following sucrose limitation, the activity of complex III was reduced in *etfqo*-1 cells. Similar behavior was observed in mutant cells when we investigated the activity of complex IV (Figure 3D). As observed for the mutant, wild type cells also presented a reduction of the activity of the complex IV. In medium without sucrose but

supplemented with BCAA, it was observed a relatively small increase of the activity of complex IV in wild type cells. Under the same condition, but for mutant cells, we did not detect any change in the activity of Complex IV.

It should be mentioned here that, in general, the absence of ETFQO protein resulted in increased activities of complex I and II in all conditions analyzed. Interestingly a reduction in the activities of complex III and IV was observed following sucrose limitation. That being said, even in cell culture supplemented with BCAAs, increased in the activities of complex III and IV were not observed in mutant cells

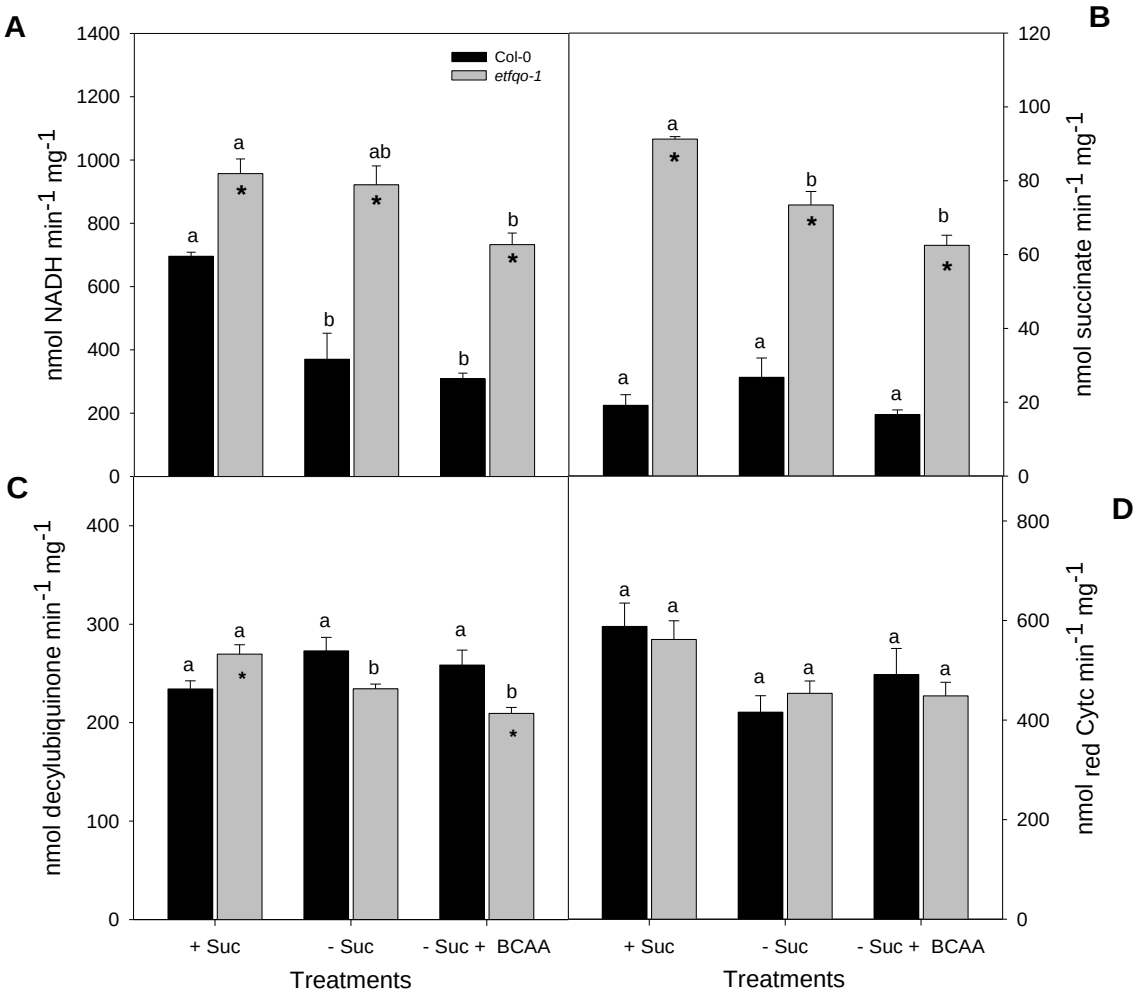

Figure 3. Activity of the oxidoreductase complexes of the respiratory chain in wild type and *etfqo*-**1. (A)** Activity of the complex I**; (B)** Activity of complex II**; (C)** Activity

of complex III**; (D)** Activity of complex IV. Assays were carried out as decribed in Material and methods using mitochondrial fractions after 24h in the three different conditions. Values are presented as means ± SE of three biological replicates. The same letters indicates no difference significant (P < 0.05, Tukey's test) between treatments for each genotype. The asterisk indicates difference significant (P < 0.05) determined by Student's *t*-test in the same treatment for each genotype. Legend: + Suc, plus sucrose; - Suc, no sucrose; - Suc + BCAA, no sucrose plus 30 mM of BCAA.

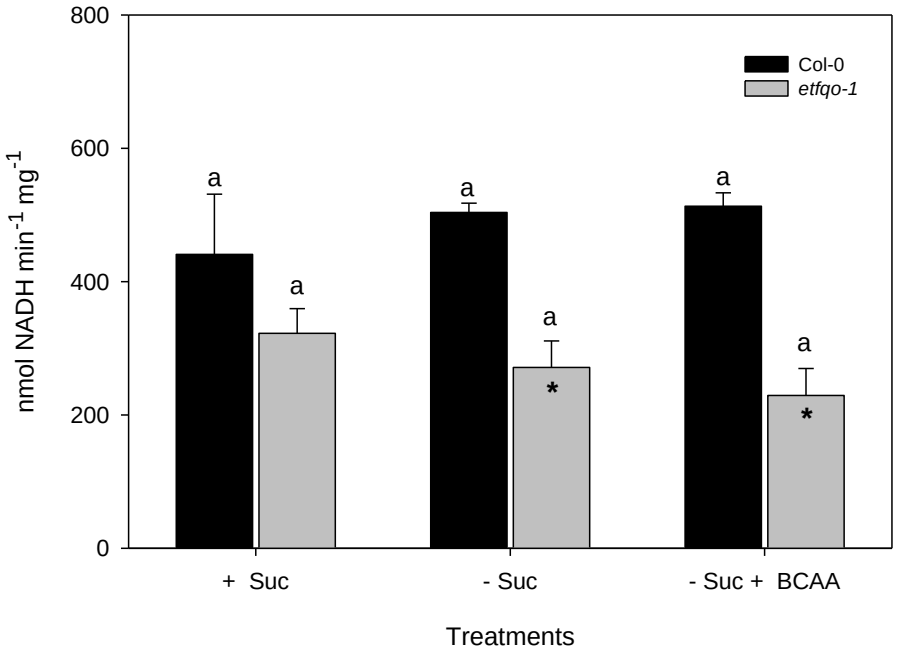

Figure 4. Alternative NADH dehydrogenases activity upon cultivation of Arabidopsis cell suspensions after 24h in the three different conditions as measured by photometric enzyme activity assays. Assays were carried out as decribed in Material and methods using mitochondrial fractions. Values are presented as means ± se of three biological replicates. The same letters indicates no difference significant (P < 0.05, Tukey's test) between treatments for each genotype. The asterisk indicates difference significant (P < 0.05) determined by Student's *t* test in the same treatment for each genotype. Legend: + Suc, plus sucrose; - Suc, no sucrose; - Suc + BCAA, no sucrose plus 30 mM of BCAA.

Isovaleryl-CoA dehydrogenase activity is not induced following carbohydrate starvation in *etfqo* mutant

To gain further insights into the functional linkage between the ETF/ETFQO system and the mitochondrial electron transport chain activities we next analyzed the activity of the Isovaleryl-CoA dehydrogenase (IVDH), since it is known that this enzyme is induced under carbon starvation (Ishizaki et al., 2005; Ishizaki et al., 2006). It was observed that the IVDH activity was induced under carbohydrate starvation in wild type cells (Figure 5A). By contrast, analyzing the IVDH activity in *etfqo-1* cells no significant alteration were observed under neither sucrose deprivation nor treatment no sucrose plus BCAA.

To further investigate whether the enzyme activity was correlated with the protein amount, we performed an immunoassay for IVDH. The results showed that increased activity was associated with significant amounts of protein in wild type cell following sucrose limited conditions (Figure 5B). Similar results were observed for cells treated with only BCAA. On the other hand, it was only detected trace amounts of IVDH in *etfqo*-1 cells under all conditions here analyzed (Figure 5B).

Enzymes involved with alternative pathways of respiration are induced following carbohydrate starvation

Given the importance of BCAA as alternative source of carbon to respiration, we next used a sensitive qRT-PCR approach to obtain a comprehensive picture of how BCAA supplementation in cell suspension cultures may affect the expression of genes involved with alternative respiration when cells are sucrose depleted and the importance of BCAA to this behavior. We selected four genes involved in the alternative respiratory pathway and that were well known associated to the ETF/ETFQO pathway. The expression of those selected genes (ETFQO, ETFβ, IVDH, and D2HGDH) was determined in cell suspensions after 3h to up to seven days following carbohydrate starvation. Our results show that the induction of expression of *ETFQO*, *IVDH* and *D2HGDH* genes occur after 6h under carbohydrate

starvation (Figure 6). By contrast, transcripts levels of ETFβ presented little, if any, changes during the time course analyzed in all treatments as previously observed by Ishizaki et al., 2005; Ishizaki et al., 2006).

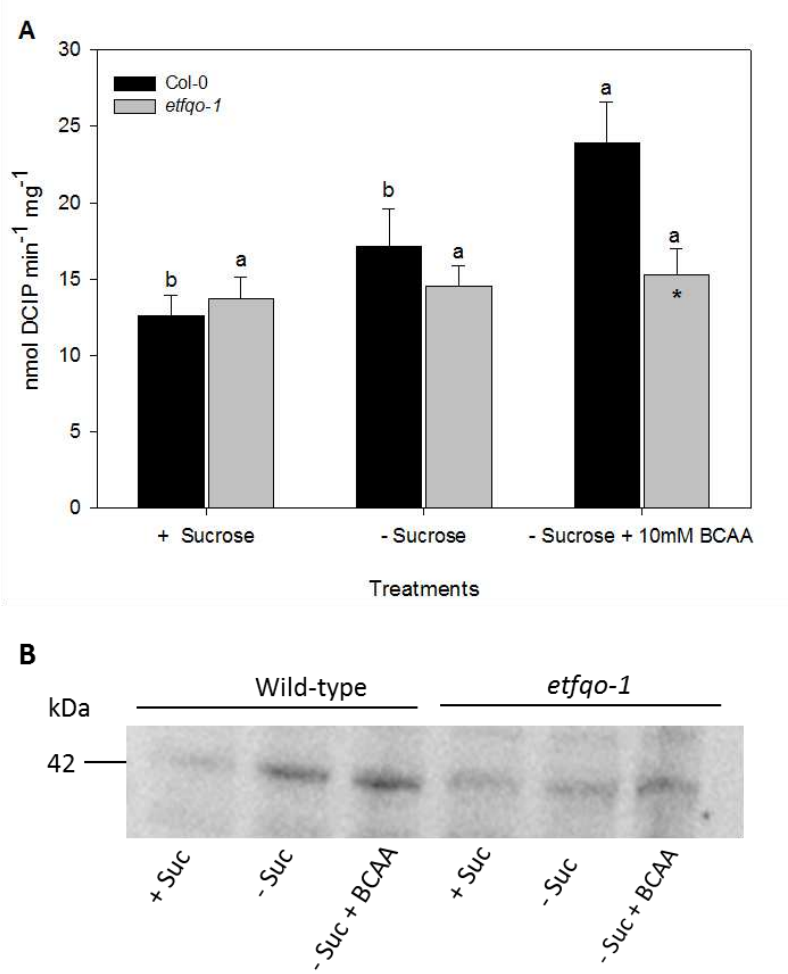

Figure 5. Isovaleryl CoA dehydrogenase activity (IVDH). **(A)** The activity of mitochondrial IVDH. Was measured in mitochondria isolated from cells of *Arabidopsis thaliana* by photometric assay. Method of determining the IVDH activity was based on the reduction of the artificial electron acceptor 2,6 dichloroindophenol (DCIP) at 600nm. Was used 20 µg of protein from soluble fraction. **(B)** Immunological detection of Isovaleryl CoA dehydrogenase (IVDH) protein in mitochondria isolated from cell suspensions cultures of the wild type and the *etfqo-1* mutants. In each well was applied 15uL of sample (each sample with 15ug of protein from soluble fraction). Was used 5ul of marker. The primary antibody IVDH was diluted as recommended 1:800 and the second antibody (Goat AR-Rabbit HRP Conjugated was diluted 1:10000.

Molecular weight to IVDH: ±45kDa (Tair Arabidospsis home). Standard errors are based on three biological replicates. Black bars represents Col-0 (wild type) and grey bars the mutants to *ETFQO-1* gene. The same letters indicates no difference significant (P < 0.05, Tukey's test) between treatments for each genotype. The asterisk indicates difference significant (P < 0.05) determined by Student's *t* test in the same treatment for each genotype. Legend: + Suc, plus sucrose; - Suc, no sucrose; - Suc + BCAA, no sucrose plus 30 mM of BCAA.

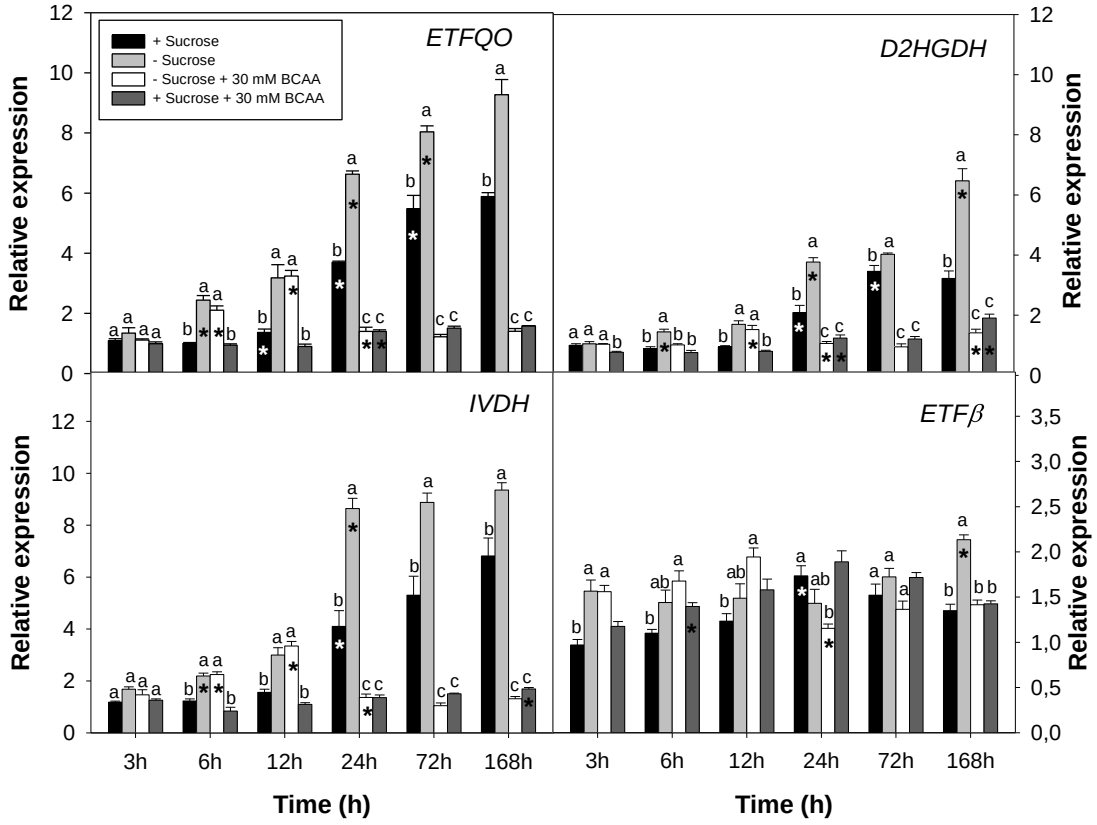

Figure 6. Transcript Levels of genes related to alternative pathways of respiration in cells suspension from *Arabidopsis thaliana.* The mRNAs were measured by quantitative RT-PCR after 3h, 6h, 12h, 24h, 72h and 168h under different conditions. Values are presented as means ± se of three biological replicates. The same letters indicates no difference significant (P < 0.05, Tukey's test) between treatments same condition. The asterisk indicates difference significant (P < 0.05) determined by Student's *t* test in the same treatment in the different times point. *F-box* was employed as a reference gene.

DISCUSSION

It has been shown that ETF/ETFQO system, one recently accepted alternative pathway of plant respiration, is induced under several environmentally and developmentally associated stress conditions that eventually lead to a restriction in the provision of carbon for mitochondrial respiration. It should be pointed. However, that this occurs concomitantly with an increase in protein degradation and amino acid metabolism (Araújo et al., 2010; Araújo et al., 2011b; Engqvist et al., 2011). Importantly, these metabolites can be further used by this complex to sustain mitochondrial respiration and the maintenance of ATP synthesis during long-term shortage of carbohydrates (Gu et al., 2010; Kochevenko et al., 2012). Therefore, this complex seems to be essential for plants to survive in sucrose limitation (Ishizaki et al., 2005; Ishizaki et al., 2006). In good agreement with this hypothesis, recent studies (Pires et al 2016) coupled with the main results obtained there demonstrated that this alternative pathway is clearly of pivotal importance for plant survival particularly under energetic stress situation. Our results demonstrated that the ETFQO activity is important for the correct activity (and ultimately) function of this alternative pathway as can be observed by the lack of induction of IVDH (Figure 5).

Our current understanding about metabolic reprogramming within respiratory metabolism as well as the responses of alternative pathways of respiration and the usage of amino acid as energy source under substrate deficiency remains rather limited (Hildebrandt et al., 2015). Here, we had performed an extensive investigation of mitochondrial metabolic aspects to further elucidate how exactly the OXPHOS system is reorganized following sucrose depletion as well as to define the key role of BCAA as alternative substrates to the mitochondrial electron transport chain. To this end, an *Arabidopsis* cell suspension was generated using mutants for the *ETFQO* gene. We decided to use *Arabidopsis* cell suspension due to its uniformity, homogeneity and repeatability that offers ideal characteristics for the study of cellular responses, particularly mitochondrial ones, getting faster and uniform results.

It has been previously reported that genes involved in the BCAA catabolism are remarkably upregulated upon sucrose starvation (Contento et al., 2004; Wang et al., 2007) (Figure 6). In addition, recent studies revealed that IVDH was play a key role in plant survival in energy-limited conditions (Ishizaki et al., 2005; Araújo et al., 2010). That being said, other enzymes involved in the BCAA catabolism might be important for plant survival and further studies are required to unequivocally demonstrate the importance of this pathway for both plant survival and mitochondrial related metabolism. By assuming the importance of this pathway and specifically of this enzyme, we carried out IVDH activity and expression analyzes. As it could be expected, IVDH activity was induced in carbon limitation conditions in wild type cells (Figure 5A) coupled with induction of this gene expression (Figure 6). Sugar starvation is known to induce degradation of proteins (Araújo et al., 2010) and the catabolism of not only fatty acids (Dieuaide et al., 1992) but also amino acids (Hildebrandt et al., 2015). It should be also mentioned, that in presence of BCAA we observed here an induction on IVDH activity substantially higher than in absence of carbohydrate (Figure 5A). These results are in good agreement with previous studies (Daschner, 2001; Araújo et al., 2010; Gu et al., 2010). Notably, by disrupting the alternative pathway of respiration involved with the usage of BCAA, as in *etfqo-1* cell cultures, no changes were observed in respect with the IVDH activity (Figure 5A). Importantly, despite the addition of BCAA to the medium, neither the enzyme activity or expression was activated, suggesting a regulatory control of ETF/ETFQO in this alternative pathway. Previous studies demonstrated that isovaleryl-CoA, substrate of the IVDH, is accumulated in mutants associated with this alternative pathway such as *etfqo* (Ishizaki et al., 2005) and ***etfβ*** (Ishizaki et al., 2006) suggesting that disruption of the last steps of this pathway most likely culminate with an impaired functioning of the IVDH. Disruption of the electron transfer function presumably compromises dehydrogenases activity and leads to accumulation of its substrate (Ishizaki et al., 2006). Moreover, it has been recently demonstrated by metabolic modeling that concentrations of intermediates upstream of a blocked reaction normally increase while those downstream of the block decrease (Ding et al., 2012). Interestingly, our immunoblotting assays showed that the increase of IVDH activity is correlated with

enhancement of IVDH protein amount in wild type cells (Figure 5B). Collectively, these findings suggest that post-translational modifications are not directly involved, but that feedback regulations is probably associated with the regulation of this pathway, what clearly deserves further studies. Transcripts of IVDH gene accumulated during carbohydrate starvation in wild type cell cultures (Figure 6) as also reported previously (Buchanan-Wollaston et al., 2005; Ishizaki et al., 2005), suggesting that carbon deprivation is able to prompt IVDH transcription. Our results indicate that the in absence of a functional ETF/ETFQO pathway, due a loss-of-function of ETFQO protein, culminates with a differential metabolic regulation of this alternative pathway, as observed for the IVDH. Thus, the results obtained here, clearly indicates a direct involvement of the ETFQO enzyme in an electron transfer chain from IVDH to ubiquinone via ETF and these electrons comes from of the degradation of BCAA.

As previously describe (Ishizaki et al., 2005; Ishizaki et al., 2006; Kleessen et al., 2012), IVDH is capable of providing electrons to the ubiquinone pool via ETF/ETFQO complex using BCAA as source of electrons. Nevertheless, this enzyme was not induced in *etfqo* mutants. Thus, our results suggest that respiration and consequently the alternative electron transfer seems be compromised in *etfqo* mutants, as demonstrated by the oxygen measurements (Table 1). Further, these results coupled with previous observation on the function of this alternative pathway (Pires et al., 2016; Araújo et al., 2010; Klossing et al., 2015) clearly open up further interesting questions regarding the consequences in the respiration in these mutants under sucrose starvation as well as in the presence of BCAA. Thereby, by performing oxygen consumption measurements in cell cultures of mutants plants in presence or absence of BCAA, we demonstrated the importance of this alternative pathway as it can be deduced by the oxygen consumption rates in wild-type cells (Table 1), that was reduced to about 50% in sucrose-free medium. It is important to mention that in *etfqo* mutants the respiration was reduced in virtually all treatments. Intriguingly, despite the addition of BCAA, cell respiration was still lower compared with that one obtained in sucrose-free medium in *etfqo* cells. Our results clearly indicated a pivotal role of BCAA catabolism within energetic stress conditions; however, it is still not clear what

are the exact roles of BCAA in the maintenance of the respiration in cells following carbohydrate starvation. Further studies should concentrate in the role of BCAA as the signaling of gene expression, as demonstrated by leucine, at least partially, in the work of Caldana et al. (2011), as well as how exactly these amino acids can drive metabolic changes in cell following carbohydrate starvation.

Recent studies using metabolic profiling of *Arabidopsis* mutants impaired in the enzymes involved with alternative respiration, such as IVDH, ETFQO, D2HGDH, demonstrated that this alternative pathway is rather crucial for respiration under extended darkness, or in other words, under carbohydrate limitation (Ishizaki et al., 2005; Ishizaki et al., 2006; Araújo et al., 2010). Notably, these studies showed an increase in the levels of various amino acids involved with starvation-induced protein degradation. Accordingly, it was also found significantly increase in the levels of GABA and TCA cycle intermediate (Araújo et al., 2010; Araújo et al., 2011a), as succinate, whereas both metabolites are not directly product of protein degradation. Metabolic and transcriptional analyses demonstrated that in plants following starvation conditions significant increase in SSADH expression are usually observed, implying an induction of the GABA catabolism bypass under these situations (Caldana et al., 2011). Despite the succinate accumulation in starved plants which may be explained by its usage as an electron donor in the respiratory chain, the role of GABA in plants is not yet fully understood. It is seems reasonable to assume this metabolite as an important signaling metabolite under times of stress (Bouché and Fromm, 2004; Fait et al., 2008; Michaeli and Fromm, 2015). Given the above evidences, the occurrence of this alternative pathway could explain, at least in part, the changes observed in the activity of complex I and II of the mETC for *etfqo* mutants (Figures 3).

In addition, we observed only virtually differences in both genotypes that presented practically the same behavior in their fresh weight in all conditions tested in this study (Figure 2). We observed that the cells grown on sucrose-free medium showed a less fresh weight. Interestingly, when sucrose or BCAA is provide as a source of carbon skeletons the fresh weight of cells increased. Autophagic mechanisms, in the first 24h after the onset of starvation, can been induced in *A. thaliana* suspension-cultured cells by carbon starvation, which

triggered an arrest of cell growth concomitantly with a rapid degradation of cellular proteins. During sucrose starvation, it is been demonstrated that the occurs the formation of autophagosome and degradation of cytoplasmic materials in cultured plant cells (Rose et al., 2006) contributing, partially, to the increase of free amino acid pools including free BCAAs to supply nutrients under this conditions (Wada et al., 2009; Izumi et al., 2010).

CONCLUSIONS

In summary, the findings presented here demonstrated that there is a strong correlation between IVDH activity and protein amount detected by immune assays. Most interesting is the fact that the activities of the mETC for both mutant and wild type were differently affected in response to carbohydrate starvation likewise by the amino acid supplied in the medium. These results suggest that ETF/ETFQO system is the main entrance of electrons by alternative dehydrogenases. However, due to the mitochondrial respiratory complex activity behavior, our results indicates that there are other entry points that may be involved within electron transfer and that particularly under stressful conditions alternative pathways of respiration are of fundamental significance. This metabolic significance although demonstrated here, remains rather unclear and therefore, in order to further elucidate the function of the enzymes of alternative respiration in land plants, further biochemical and metabolic studies should be performed and thus may provide new metabolic insights into the alternative respiration in plants.

REFERENCES

Araújo WL, Ishizaki K, Nunes-Nesi A, Larson TR, Tohge T, Krahnert I, Witt S, Obata T, Schauer N, Graham I a, et al (2010) Identification of the 2-hydroxyglutarate and isovaleryl-CoA dehydrogenases as alternative electron donors linking lysine catabolism to the electron transport chain of Arabidopsis mitochondria. Plant Cell **22**: 1549–63

Araújo WL, Ishizaki K, Nunes-Nesi A, Tohge T, Larson TR, Krahnert I, Balbo I, Witt S, Dörmann P, Graham I a, et al (2011a) Analysis of a Range of Catabolic Mutants Provides Evidence That Phytanoyl-Coenzyme A Does Not Act as a Substrate of the Electron-Transfer Flavoprotein/Electron-Transfer Flavoprotein:Ubiquinone Oxidoreductase Complex in Arabidopsis during Dark-Induced Sene. Plant Physiol **157**: 55–69

Araújo WL, Tohge T, Ishizaki K, Leaver CJ, Fernie AR (2011b) Protein degradation - an alternative respiratory substrate for stressed plants. Trends Plant Sci. doi: 10.1016/j.tplants.2011.05.008

Birch-Machin MA, Briggs HL, Saborido AA, Bindoff LA, Turnbull DM (1994) An Evaluation of the Measurement of the Activities of Complexes I-IV in the Respiratory Chain of Human Skeletal Muscle Mitochondria. Biochem Med Metab Biol **51**: 35–42

Bouché N, Fromm H (2004) GABA in plants: Just a metabolite? Trends Plant Sci **9**: 110–115

Bradford MM (1976) A rapid and sensitive method for the quantitation of microgram quantities of protein utilizing the principle of protein-dye binding. Anal Biochem **72**: 248–254

Buchanan-Wollaston V, Page T, Harrison E, Breeze E, Lim PO, Nam HG, Lin JF, Wu SH, Swidzinski J, Ishizaki K, et al (2005) Comparative transcriptome analysis reveals significant differences in gene expression and signalling pathways between developmental and dark/starvation-induced senescence in Arabidopsis. Plant J **42**: 567–585

Caldana C, Degenkolbe T, Cuadros-Inostroza A, Klie S, Sulpice R, Leisse A, Steinhauser D, Fernie AR, Willmitzer L, Hannah MA (2011) High-

density kinetic analysis of the metabolomic and transcriptomic response of Arabidopsis to eight environmental conditions. Plant J **67**: 869–884

Contento AL, Kim S-J, Bassham DC (2004) Transcriptome profiling of the response of Arabidopsis suspension culture cells to Suc starvation. Plant Physiol **135**: 2330–2347

Daschner K (2001) The Mitochondrial Isovaleryl-Coenzyme A Dehydrogenase of Arabidopsis Oxidizes Intermediates of Leucine and Valine Catabolism. Plant Physiol **126**: 601–612

Dieuaide M, Brouquisse R, Pradet A, Raymond P (1992) Increased Fatty Acid beta-Oxidation after Glucose Starvation in Maize Root Tips. Plant Physiol **99**: 595–600

Ding G, Che P, Ilarslan H, Wurtele ES, Nikolau BJ (2012) Genetic dissection of methylcrotonyl CoA carboxylase indicates a complex role for mitochondrial leucine catabolism during seed development and germination. Plant J **70**: 562–577

van Dongen JT, Gupta KJ, Ramírez-Aguilar SJ, Araújo WL, Nunes-Nesi A, Fernie AR (2011) Regulation of respiration in plants: A role for alternative metabolic pathways. J Plant Physiol **168**: 1434–1443

Engqvist M, Drincovich MF, Flügge UI, Maurino VG (2009) Two D-2-hydroxy-acid dehydrogenases in arabidopsis thaliana with catalytic capacities to participate in the last reactions of the methylglyoxal and β-oxidation pathways. J Biol Chem **284**: 25026–25037

Engqvist MKM, Kuhn A, Wienstroer J, Weber K, Jansen EEW, Jakobs C, Weber APM, Maurino VG (2011) Plant D-2-hydroxyglutarate dehydrogenase participates in the catabolism of lysine especially during senescence. J Biol Chem **286**: 11382–11390

Fait A, Fromm H, Walter D, Galili G, Fernie AR (2008) Highway or byway: the metabolic role of the GABA shunt in plants. Trends Plant Sci **13**: 14–19

Geigenberger P, Fernie AR, Gibon Y, Christ M, Stitt M (2000) Metabolic Activity Decreases as an Adaptive Response to Low Internal Oxygen in Growing Potato Tubers. Biol Chem **381**: 723–740

Gu L, Jones AD, Last RL (2010) Broad connections in the Arabidopsis seed metabolic network revealed by metabolite profiling of an amino acid

catabolism mutant. Plant J **61**: 579–590

Heazlewood JL, Tonti-Filippini JS, Gout AM, Day DA, Whelan J, Millar AH (2004) Experimental analysis of the Arabidopsis mitochondrial proteome highlights signaling and regulatory components, provides assessment of targeting prediction programs, and indicates plant-specific mitochondrial proteins. Plant Cell **16**: 241–56

Hildebrandt TM, Nunes-Nesi A, Araújo WL, Braun H-P (2015) Amino Acid Catabolism in Plants. Mol Plant **8**: 1563–79

Ishizaki K, Larson TR, Schauer N, Fernie AR, Graham IA, Leaver CJ (2005) The critical role of Arabidopsis electron-transfer flavoprotein:ubiquinone oxidoreductase during dark-induced starvation. Plant Cell **17**: 2587–2600

Ishizaki K, Schauer N, Larson TR, Graham IA, Fernie AR, Leaver CJ (2006) The mitochondrial electron transfer flavoprotein complex is essential for survival of Arabidopsis in extended darkness. Plant J **47**: 751–760

Izumi M, Wada S, Makino A, Ishida H (2010) The Autophagic Degradation of Chloroplasts via Rubisco-Containing Bodies Is Specifically Linked to Leaf Carbon Status But Not Nitrogen Status in Arabidopsis. PLANT Physiol **154**: 1196–1209

Kirma M, Araújo WL, Fernie AR, Galili G (2012) The multifaceted role of aspartate-family amino acids in plant metabolism. J Exp Bot **63**: 4995–5001

Kleessen S, Araújo WL, Fernie AR, Nikoloski Z (2012) Model-based confirmation of alternative substrates of mitochondrial electron transport chain. J Biol Chem **287**: 11122–11131

Kochevenko A, Araújo WL, Maloney GS, Tieman DM, Do PT, Taylor MG, Klee HJ, Fernie AR (2012) Catabolism of branched chain amino acids supports respiration but not volatile synthesis in tomato fruits. Mol Plant **5**: 366–75

Laemmli UK (1970): (1970) Cleavage of Structural Proteins during Assembly of Head of Bacteriophage- T4. Nature **227**: 680–685

Lang JK, Packer L (1987) Quantitative determination of vitamine E and reduced coenzyme Q by high-performance liquid chromatography with in-line ultraviolet and electrochemical detection. J Chromatogr **385**: 109–117

Lehmann M, Schwarzländer M, Obata T, Sirikantaramas S, Burow M,

Olsen CE, Tohge T, Fricker MD, Møller BL, Fernie AR, et al (2009) The metabolic response of Arabidopsis roots to oxidative stress is distinct from that of heterotrophic cells in culture and highlights a complex relationship between the levels of transcripts, metabolites, and flux. Mol Plant **2**: 390–406

May MJ, Leaver C j (1993) Oxidative Stimulation of Glutathione Synthesis in Arabidopsis thaliana Suspension Cultures. Plant Physiol **103**: 621–627

Michaeli S, Fromm H (2015) Closing the loop on the GABA shunt in plants: are GABA metabolism and signaling entwined? Front Plant Sci **6**: 419

Millar AH, Heazlewood JL, Kristensen BK, Braun H-P, Møller IM (2005) The plant mitochondrial proteome. Trends Plant Sci **10**: 36–43

Millar AH, Whelan J, Soole KL, Day DA (2011) Organization and regulation of mitochondrial respiration in plants. Annu Rev Plant Biol **62**: 79–104

Murashige T, Skoog F (1962) A Revised Medium for Rapid Growth and Bio Assays with Tobacco Tissue Cultures. Physiol Plant **15**: 473–497

Pires M V., Pereira Júnior AA, Medeiros DB, Daloso DM, Pham PA, Barros KA, Engqvist MKM, Florian A, Krahnert I, Maurino VG, et al (2016) The influence of alternative pathways of respiration that utilize branched-chain amino acids following water shortage in Arabidopsis. Plant, Cell Environ **39**: 1304–1319

Plaxton WC, Podestá FE (2006) The Functional Organization and Control of Plant Respiration. CRC Crit Rev Plant Sci **25**: 159–198

Rose TL, Bonneau L, Der C, Marty-Mazars D, Marty F (2006) Starvation-induced expression of autophagy-related genes in Arabidopsis. Biol Cell **98**: 53–67

Schertl P, Braun H-P (2014) Respiratory electron transfer pathways in plant mitochondria. Front Plant Sci **5**: 163

Schertl P, Cabassa C, Saadallah K, Bordenave M, Savour?? A, Braun HP (2014) Biochemical characterization of proline dehydrogenase in Arabidopsis mitochondria. FEBS J **281**: 2794–2804

Wada S, Ishida H, Izumi M, Yoshimoto K, Ohsumi Y, Mae T, Makino A (2009) Autophagy Plays a Role in Chloroplast Degradation during Senescence in Individually Darkened Leaves. Plant Physiol **149**: 885–893

Wang HJ, Wan AR, Hsu CM, Lee KW, Yu SM, Jauh GY (2007)

Transcriptomic adaptations in rice suspension cells under sucrose starvation. Plant Mol Biol **63**: 441–463

Watmough NJ, Frerman FE (2010) The electron transfer flavoprotein: Ubiquinone oxidoreductases. Biochim Biophys Acta - Bioenerg **1797**: 1910–1916

Welchen E, Hildebrandt TM, Lewejohann D, Gonzalez DH, Braun H-P (2012) Lack of cytochrome c in Arabidopsis decreases stability of Complex IV and modifies redox metabolism without affecting Complexes I and III. Biochim Biophys Acta - Bioenerg **1817**: 990–1001

GENERAL CONCLUSIONS

Despite the fast advances in the last years in various molecular tools together to bioinformatics analysis, there are still some gaps in our knowledge in the metabolism of plants. The understanding on transport of metabolites as well as the regulation of the responses of alternative respiration pathway under stress are some aspects of mitochondrial metabolism that remains incomplete. For this reason, in this study, we investigated the role of two integral mitochondrial membrane proteins each one involved in one of the metabolic processes mentioned. The first one is a mitochondrial transporter of organic acids, *At*SFC1. We demonstrate that this carrier is a citrate/isocitrate transport that potentially link β-oxidation of fatty acids, glyoxylate cycle with the TCA cycle suppling these pathways with carbon skeletons. In addition, deficiency in this protein led a great effects in the growth root and photosynthesis. In concerning the second protein, ETFQO, we investigate its role in the electron transfer during carbon deprivation. The absence of ETFQO protein, in general, resulted in increased activity of complex I and II. We suggest that probably, GABA shunt is been upregulated and act as an alternative source of NADH and/or succinate for the respiratory complexes I and II, respectively. However, other entry points should be considered, which must be elucidated and provide new metabolic insights into the alternative respiration in plants.